RAFFLES BULLETIN OF ZOOLOGY **69**: 80–101
Date of publication: 15 March 2021
DOI: 10.26107/RBZ-2021-0007
http://zoobank.org/urn:lsid:zoobank.org:pub:A9E97760-A5C2-4FC1-A760-71145414B549

Two new species of *Pethia* (Teleostei: Cyprinidae), representing a sympatric species pair, from the Ayeyarwady drainage, Myanmar

Kevin W. Conway[1,2], Amanda K. Pinion[1] & Maurice Kottelat[3]

Abstract. Two new species of *Pethia*, *P. castor* and *P. pollux*, are described from flooded areas of the Ayeyarwady drainage in Kachin State and Sagaing Region, central Myanmar. The two species are largely sympatric and syntopic, generally similar in external appearance, and distinguished from congeners by the absence of black blotches (round or vertically elongate) on the body. *Pethia castor* and *P. pollux* are distinguished from each other by subtle characters of the mouth and snout, osteology, and colour pattern in preservative. The uncorrected P-distance (based on mitochondrial cytochrome c oxidase I [COI] gene sequences) between the two new species is 8.2%. Phylogenetic analyses of a small dataset of COI sequences for 16 species of *Pethia* plus outgroup taxa corroborates *Pethia* as a monophyletic group, inside of which *P. castor* and *P. pollux* represent sister taxa, and together represent the sister taxon of the Ganga-Brahmaputran *P. gelius*.

Key words. taxonomy, Cypriniformes, Smiliogastrinae, 'barbs'

INTRODUCTION

The South and Southeast Asian cyprinid genus '*Puntius*' has long been recognised as a polyphyletic assemblage (Rainboth, 1986, 1989, 1991, 1996; Kullander, 2008; Pethiyagoda et al., 2012; Kottelat, 2013). In recent years, several members of this catch-all genus have been reassigned to other genera, many of which were newly described for this purpose (e.g., Pethiyagoda et al., 2012; Kottelat, 2013). The genus *Pethia* was created by Pethiyagoda et al. (2012) to accommodate small-bodied (usually less than 60 mm SL) '*Puntius*' from South and Southeast Asia that were previously recognised as members of the *Puntius conchonius* species group (Taki et al., 1978; Kullander, 2008). Species of *Pethia* typically exhibit one or two black blotches or bars on the side of the body, including an anterior (humeral) marking and/or a posterior marking on the caudal peduncle. They differ from *Puntius* sensu stricto by having an incomplete lateral line (with exceptions), and a stiff, serrated last unbranched dorsal-fin ray (Pethiyagoda et al., 2012).

Pethia is distributed throughout South and Southeast Asia, from Sri Lanka and peninsular India in the west, to the Mekong drainage of Laos and Thailand in the east (Kottelat, 2001; Batuwita et al., 2015; Katwate et al., 2016). Several species of *Pethia* are reported from Myanmar, including *P. didi*, *P. erythromycter*, *P. expletiforis*, *P. macrogramma*, *P. meingangbii*, *P. nankyweensis*, *P. ornata*, *P. padamya*, *P. stoliczkana*, *P. thelys*, *P. tiantian*, and *P. yuensis* (see e.g., Kullander & Fang, 2005; Kullander, 2008; Kullander & Britz, 2008; Kottelat, 2015; Kottelat & Nyein Chan, 2017; Shangningam & Vishwanath, 2018). All these species exhibit a black blotch (of variable size and shape) on the caudal peduncle, and may or may not exhibit an additional black blotch or vertically elongate (humeral) marking anteriorly. The majority of the aforementioned Myanmarese species of *Pethia* are endemic to the middle and upper reaches of the Ayeyarwady, including the Chindwin, with the majority of available material in museum collections obtained from within the borders of Kachin State, and the Mandalay and Sagaing regions (Kullander & Fang, 2005; Kullander, 2008; Kullander & Britz, 2008). To the south and east of the Ayeyarwady drainage, *Pethia* is represented only by *P. stoliczkana*, which extends as far south as the Lenya River drainage in extreme southern Myanmar (Kottelat, 2015), and as far east as the Mekong drainage in northern Laos (Kottelat, 2001).

A recent survey of the Middle Ayeyarwady between Myitkyina and Mandalay (Kottelat & Nyein Chan, 2017) produced specimens of small cyprinids lacking dark markings on the body side, which could not be assigned to genus in the field and were temporarily referred to as *Puntius* sp. 'dorsal spot' (Kottelat & Nyein Chan, 2017). Subsequent examination revealed that this material represents two

Accepted by: Tan Heok Hui

[1]Department of Ecology and Conservation Biology and Biodiversity Research and Teaching Collections, Texas A&M University, College Station, TX 77843, USA; Email: kevin.conway@tamu.edu; akpinion@tamu.edu

[2]Research Associate, Ichthyology, Australian Museum Research Institute, 1 William Street, Sydney, NSW 2010, Australia

[3]Rue des Rauraques 6, 2800 Delémont, Switzerland (permanent address); and Lee Kong Chian Natural History Museum, National University of Singapore, 2 Conservatory Drive, Singapore 117377; Email: mkottelat@dplanet.ch

ISSN 2345-7600 (electronic) | ISSN 0217-2445 (print)

undescribed species of *Pethia* which, however, lack dark markings on the body. In this paper, we describe these two distinct 'plain' species of *Pethia* and comment on their putative phylogenetic placement within the genus based on a phylogenetic analysis of Cytochrome Oxidase Subunit I (COI) sequences.

MATERIAL AND METHODS

Counts and measurements generally follow those of Kullander (2008). Specimens were measured to the nearest 0.1 mm using digital callipers. Select specimens were cleared and double stained (C&S) following the protocol of Taylor & Van Dyke (1985). Counts of fin rays and internal skeletal structures were obtained from C&S specimens. Scale counts were obtained from alcohol preserved specimens. A value in parentheses provided after a count indicates the frequency of that count (note some counts could not be obtained from all specimens examined). An asterisk (*) provided in association with a value in descriptions denotes the value obtained from holotype (if available). Observations and photographs of cleared and stained specimens or their parts were generally made using a ZEISS SteReo Discovery V20 stereomicroscope equipped with a Zeiss Axiocam MRc5 digital camera. Images were obtained using the stacking function in the Zeiss Axiovision software and processed using a combination of Adobe Photoshop 2020 and Illustrator 2020. Computed tomography (CT) scans of two paratype individuals (one of each species) were obtained at the Karel F. Liem BioImaging Center (Friday Harbor Laboratories, University of Washington) using a Bruker SkyScan 1173 scanner with a 1 mm aluminium filter. Scans were run at 65 kV and 123 µA on a 2048×2048 pixel CCD at a resolution of 9.9–12.4 µm. Specimens were scanned while inside a 50 ml plastic Falcon tube, in which they were wrapped with cheesecloth moistened with ethanol (70%) to prevent movement during scanning. The resulting CT data were visualised using 3D Slicer v.4.10.2 (https://www.slicer.org/) and have been deposited on MorphoSource (https://www.morphosource.org/). Osteological terminology used herein follows that of Conway (2011), except that we use mesethmoid instead of ethmoid complex.

DNA was extracted from fin clips of select specimens using a DNeasy Tissue Extraction Kit (Qiagen, Inc., Valencia, CA, USA) following the manufacturer's protocols. The cytochrome c oxidase subunit I gene (COI) was amplified using the primer pair LCO-1490 and HCO-2198 (Folmer et al., 1994). All PCR amplifications were conducted in 25 µl reactions containing 12.5 µl EmeraldAmp GT PCR Master Mix (Takara, Japan), 10.7 µl nuclease-free water, 1 µl (300 ng) of template DNA, and 0.4 µl of each primer (forward and reverse). PCR conditions included initial denaturation at 94°C for 4 min, then 35 cycles at 94°C for 30 s each, 41°C for 30 s, and 72°C for 1 min, followed by a final extension at 72°C for 10 min. Amplified PCR product was sequenced by Macrogen (Rockville, MD, USA) in both directions using the PCR primers as sequencing primers. Sequences have been deposited in GenBank under the accession numbers provided in Appendix 1. Genetic distance (uncorrected P-distance) between COI sequences obtained from individuals of the new species were calculated using MegaX (Kumar et al., 2018; Stecher et al., 2020).

To investigate the phylogenetic position of the new species we conducted a Maximum Likelihood (ML) and Maximum Parsimony (MP) analysis of a data set comprising 664 bp of COI for 64 individuals, representing 16 species of *Pethia* and 23 outgroup taxa (following Katwate et al., 2016). Sequences, other than those generated as part of this study, were obtained from GenBank (see Appendix 1). Sequences were aligned by eye using BBEdit v.12.1.5 (Bare Bones Software Inc.). The final aligned data set was analysed using ML criteria as implemented in GARLI v.2.01 (Zwickl, 2006) and MP criteria as implemented in PAUP* v.4.0a (build 168) (Swofford, 2003). For ML analyses, we conducted 100 bootstrap replicates and searched for the best scoring ML tree simultaneously in a single analysis with all parameters set to default. The resulting best scoring ML phylogram was rooted with *Garra* and viewed using FIGTREE v.1.4.4 (http://tree.bio.ed.ac.uk/software/figtree). For MP analyses, we used heuristic searches, utilising tree-bisection and reconnection (TBR) branch swapping, with starting trees obtained by random stepwise addition (# reps 100). The maximum number of trees saved during each run was allowed to automatically increase by 100, and the MULTREES option was in effect. All characters were equally weighted and unordered. Nodal support was estimated using non-parametric bootstrapping (Felsenstein, 1985) for 1000 pseudoreplicates, using "fast" step-wise addition. Resulting equally parsimonious cladograms were rooted using *Garra*, summarised using a strict consensus method and viewed using FIGTREE v1.3.1.

Collection abbreviations used: CMK, collection of Maurice Kottelat, Delémont, Switzerland; MHNG, Muséum d'Histoire Naturelle, Geneva, Switzerland; TCWC, Collection of Fishes, Biodiversity Research and Teaching Collections, Texas A&M University, College Station, USA; UF, Florida Museum Fish Collection, University of Florida, Gainesville, USA; ZRC, Lee Kong Chian Natural History Museum, National University of Singapore, Singapore.

TAXONOMY

Pethia castor, new species

(Fig. 1)

Holotype. MHNG 2785.033, 36.9 mm SL; Myanmar: Kachin State: mouth of outlet of Indaw Inn into Ayeyarwady River, 24°13′08″N 96°49′25″E [near Shwegu]; M. Kottelat & Nyein Chan, 27 June 2017.

Paratypes. Myanmar: Kachin State: CMK 27085, 24, 38.4–39.7 mm SL; ZRC 61662, 8, 35.0–37.5 mm SL; TCWC 20251.01, 1 [CT voucher, M87960], 34.7 mm SL; TCWC 20251.02, 8, 34.5–37.9 mm SL; TCWC 20251.03, 2 [C&S], 36.0–38.4 mm SL; same as holotype. — CMK 28806, 2,

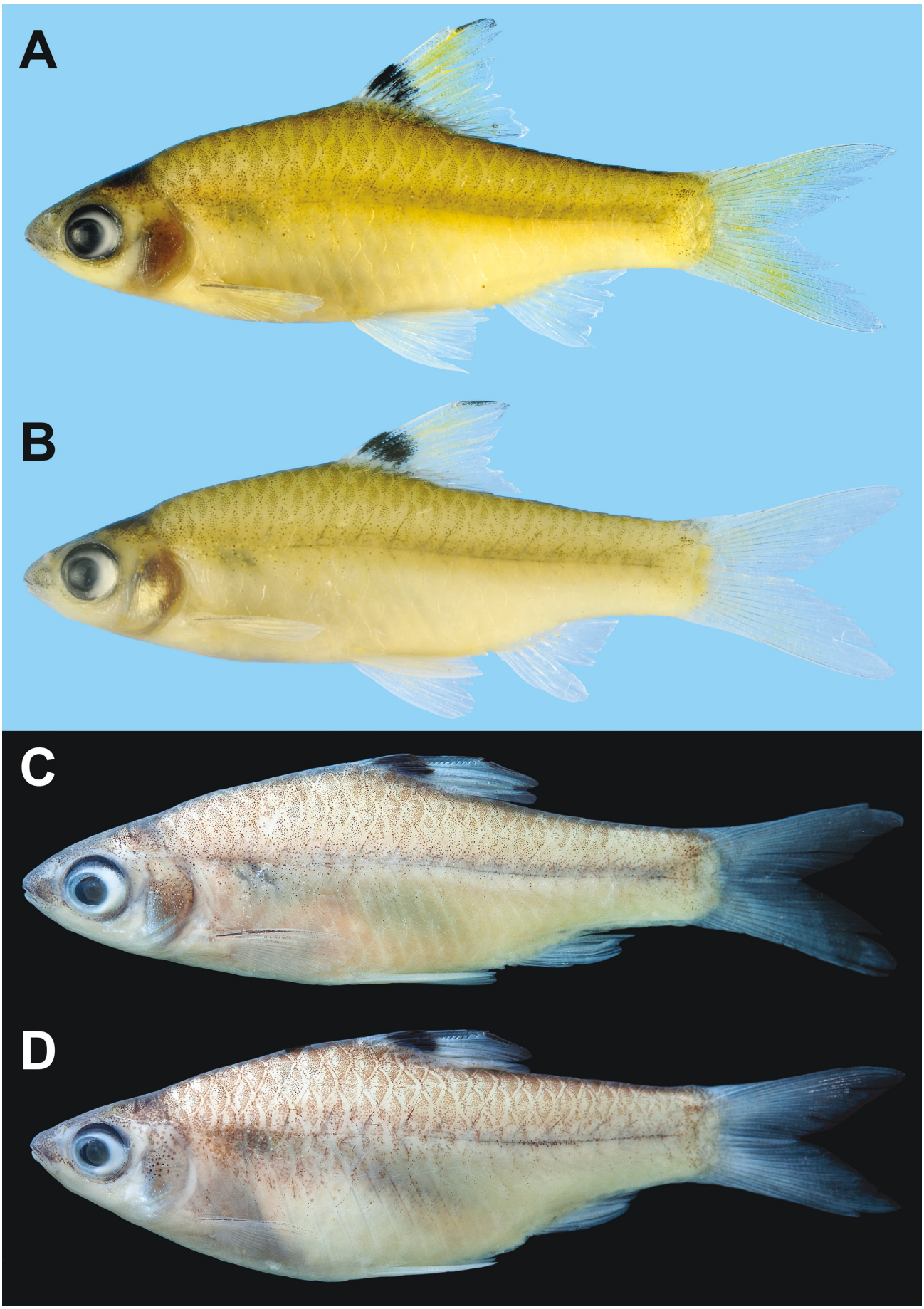

Fig. 1. *Pethia castor*, Myanmar, Sagaing Region (A, B, photographed after short period in formalin) and Kachin State (C, D). **A**, CMK 27159, paratype, male, 38.6 mm SL; **B**, CMK 27130, paratype, male, 39.4 mm SL; **C**, CMK 27085, paratype, male, 35.2 mm SL; **D**, MHNG 2785.033, holotype, female, 36.9 mm SL.

29.7–35.5 mm SL; 2, 35.7–38.4 mm SL [DNA voucher, fixed in 95% ethanol]; Tan Pway Kone Chaung at northern edge of Thila Pha Inn, Indaw Inn, 24°18′15″N 96°48′42″E [near Shwegu]; M. Kottelat & Nyein Chan, 27 June 2017.

Other Material. Myanmar. **Sagaing Region:** CMK 27130, 1, 39.4 mm SL; Ayeyarwady River upstream of Hti Chaint, 23°46′23″N 96°10′22″E; M. Kottelat & Nyein Chan, 30 June 2017. — CMK 27144, 2, 32.4–34.5 mm SL; Ayeyarwady River upstream of Hti Chaint, Sa Khan Kyaut Maw Inn (backwaters), 23°46′23″N 96°10′22″E; M. Kottelat & Nyein Chan, 30 June 2017. — CMK 27159, 5, 35.4–39.9 mm SL; Ayeyarwady River near Hti Chaint Myit Yoe, 23°43′59″N 96°09′50″E; M. Kottelat & Nyein Chan, 30 June 2017. — CMK 27224, 1, 35.4 mm SL; Ayeyarwady River, sand bank near Shein Ma Kar village, about 40 km North of Mandalay, 22°18′20″N 95°59′12″E; M. Kottelat et al., 2 July 2017. — CMK 28787, 113, 26.7–42.2 mm SL; same data as holotype.

Diagnosis. *Pethia castor* is distinguished from all other species of *Pethia*, except *P. pollux*, by the absence of black blotches (round or vertically elongate) on the body, and by the presence of two black markings on anterior half of dorsal fin, including a larger marking over base of second unbranched to third branched ray and intervening fin membranes, and a smaller marking covering the distal, flexible tip of third unbranched ray.

The external differences in preserved material of *P. castor* and *P. pollux* are not striking and may not be discernible in specimens that have not been optimally preserved. *Pethia castor* is distinguished from *P. pollux* by the weak horizontal stripe along body side (most evident in males; Fig. 1A–C) (vs. absence); scales on lower half of caudal peduncle with few or no faint brown melanophores scattered over pocket and along posterior margin, when present forming a weak or barely discernible reticulate pattern (vs. with dense scattering of dark brown melanophores, forming an obvious reticulate pattern; Fig. 2A); the absence of isolated lateral-line canal ossicles on scales in lateral-line canal row on posterior part of body (vs. presence); a slightly shorter (19–25% HL vs. 23–29), more rounded (vs. pointed) snout; a slightly smaller eye (orbit diameter 29–33% HL vs. 32–36); upper lip relatively thin, of uniform thickness along lateral margin of jaw (vs. upper lip swollen posteriorly); lateral fold on snout poorly developed (vs. well developed) along anterior margin of lachrymal; rostral cap barely discernible from remainder of snout, not overlapping upper lip dorsally (vs. rostral cap swollen, obvious in lateral view, overlapping upper lip at midline).

The following osteological characters too, distinguish *P. castor* from *P. pollux*: ascending process of premaxilla poorly developed, posteriormost tip not reaching midpoint of kinethmoid with jaws closed (vs. ascending process moderately developed, posteriormost tip reaching past midpoint of kinethmoid with jaws closed); posterior part of anguloarticular elevated dorsally as large triangular process (vs. posterior part of anguloarticular with flat dorsal margin); central part of mesethmoid weakly concave (vs. with central cavernous indentation); supraorbital relatively narrow anteriorly, tapering in width gently towards posterior, firmly attached to lateral ethmoid anteriorly (vs. relatively wide anteriorly, tapering in width abruptly towards posterior, not in contact with lateral ethmoid anteriorly); anterior edge of epibranchial 1 with well-developed (vs. poorly developed), shelf-like anterior extension.

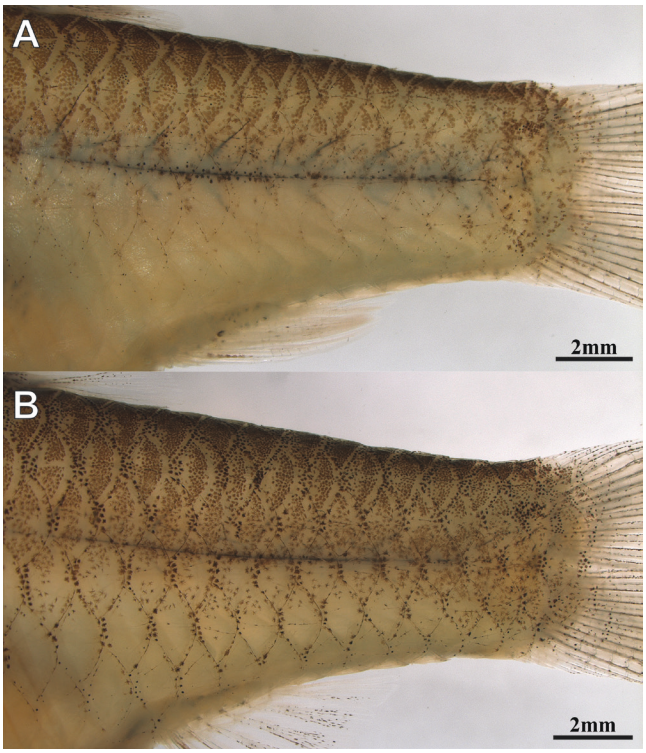

Fig. 2. Pigmentation pattern on caudal peduncle scales in *Pethia*. **A**, *P. castor*, MHNG 2785.033, holotype, female, 36.9 mm SL; **B**, *P. pollux*, MHNG 2785.034, holotype, female, 40.4 mm SL.

Description. See Figure 1 for general appearance and Table 1 for morphometric data obtained from holotype and 9 paratypes. Body laterally compressed, relatively deep, greatest depth at dorsal-fin origin. Caudal peduncle depth approximately equal to head depth through mid-orbit. Dorsal profile continuous between head and body, with slight hump at nape, ascending, almost straight prior to dorsal fin, descending almost straight from dorsal-fin origin to just anterior of base of caudal fin, slightly concave at base of caudal fin. Ventral profile of head and body continuous, rounded through pelvic- and anal-fin bases, slightly concave along caudal peduncle.

Head short, laterally compressed (Fig. 3). Eye diameter greater than snout length. Pupil spherical to subelliptical (Fig. 3A, B). Snout rounded to moderately pointed (Fig. 3A) in lateral aspect. Mouth small, subterminal, not reaching vertical through anterior margin of anterior nostril. Lips exposed, smooth, moderately thick; lower lip fold interrupted medially. Lateral fold on snout poorly developed, located along anterior margin of lachrymal. Rostral cap poorly developed (Fig. 3B). Barbels absent. Skin anterior to eye thick, depigmented, opaque (Fig. 3B), visible in dorsal view as a clear, slightly bulbous patch of opaque skin between

Table 1. Morphometric characters of *Pethia castor* (10 total, including holotype and 9 paratypes from TCWC 20251.02) and *P. pollux* (10 total, including holotype, 3 paratypes from CMK 27070, 2 from CMK 28804, and 4 from TCWC 20250.02). Range values include value obtained from holotype.

	Pethia castor				*Pethia pollux*			
	Holotype	**Range**	**Mean**	**St. Dev.**	**Holotype**	**Range**	**Mean**	**St. Dev.**
Standard Length	36.9	33.9–39.4	–	–	41.2	33.0–41.2	–	–
In percent of the standard length								
Head length	26.9	26.3–28.9	27.4	0.7	27.2	26.9–30.2	28.3	1.1
Body depth	34.0	29.9–34.8	32.4	2.1	34.5	30.2–34.5	32.3	1.7
Predorsal length	50.5	50.3–54.2	51.5	1.2	50.5	50.5–54.1	53.0	1.1
Prepelvic length	54.1	50.3–54.1	51.5	1.2	50.0	50.0–54.5	51.9	1.3
Preanal length	77.7	72.1–77.7	74.0	1.8	71.1	71.1–75.2	73.3	1.3
Caudal peduncle depth	13.3	13.3–15.4	14.4	0.6	14.8	13.6–14.8	14.1	0.4
Caudal peduncle length	17.9	15.3–21.1	18.8	1.7	21.1	18.6–21.3	20.4	0.9
Dorsal fin length	26.6	22.3–26.8	24.5	2.1	–	24.4–27.4	26.0	1.1
Anal fin length	15.8	14.7–18.0	16.3	1.0	14.6	13.1–15.6	14.5	0.8
Pectoral fin length	19.0	17.0–22.1	19.4	1.8	20.6	16.7–21.8	19.8	1.5
Pelvic fin length	18.5	18.8–20.4	20.4	1.2	22.1	19.4–22.3	21.2	0.9
In percent of head length								
Snout length	23	19–25	21.4	1.8	26	23–28	25.6	1.7
Eye diameter	30	29–33	31.1	1.3	35	32–36	34.5	1.4
Interorbital width	34	34–38	36.6	1.3	36	32–39	35.8	1.9
Head width	40	37–43	39.9	1.9	46	38–46	41.1	2.7
Head depth (occiput)	72	67–76	71.5	2.5	71	66–73	69.1	2.1

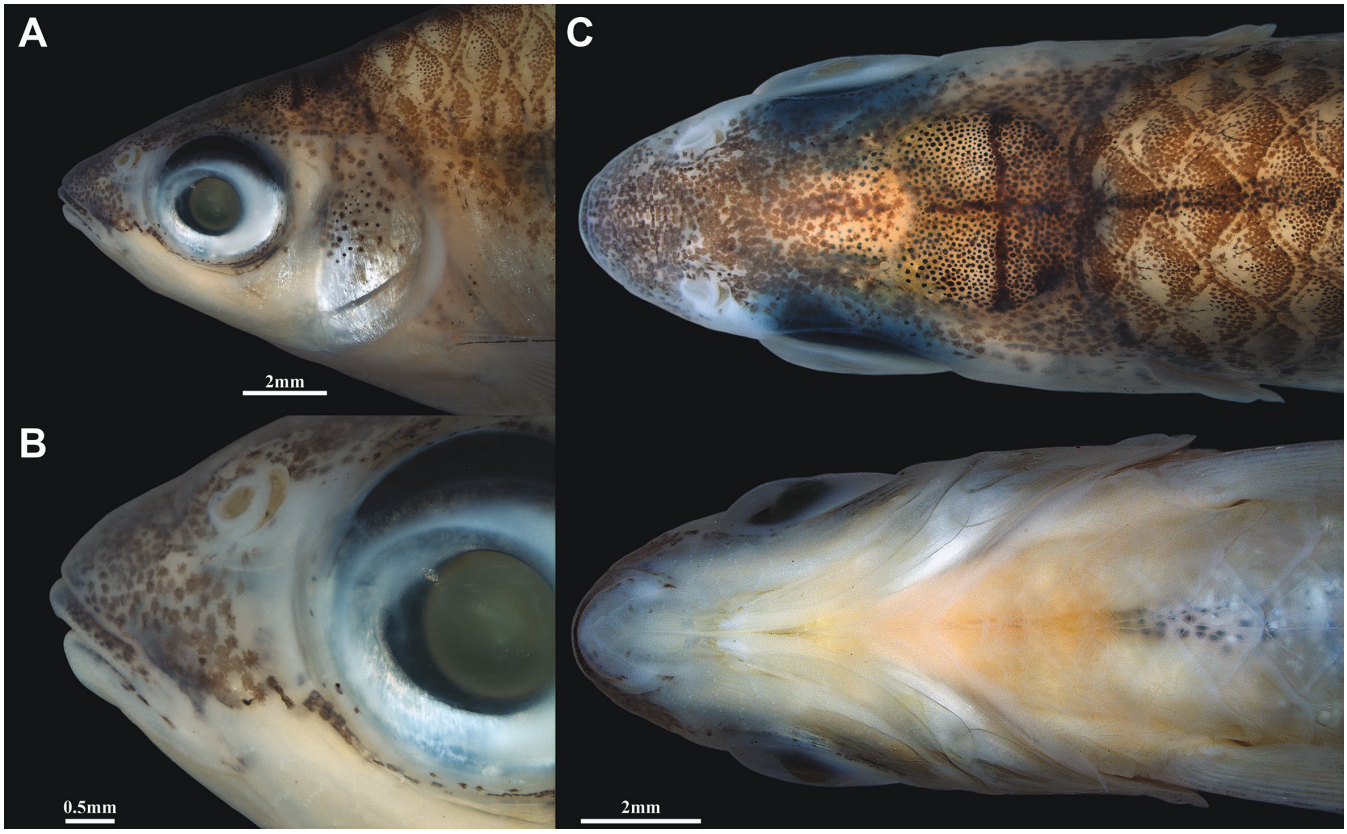

Fig. 3. *Pethia castor*, MHNG 2785.033, holotype, 36.9 mm SL; **A**, head in lateral view; **B**, close up of snout in lateral view; **C**, head in dorsal and ventral view.

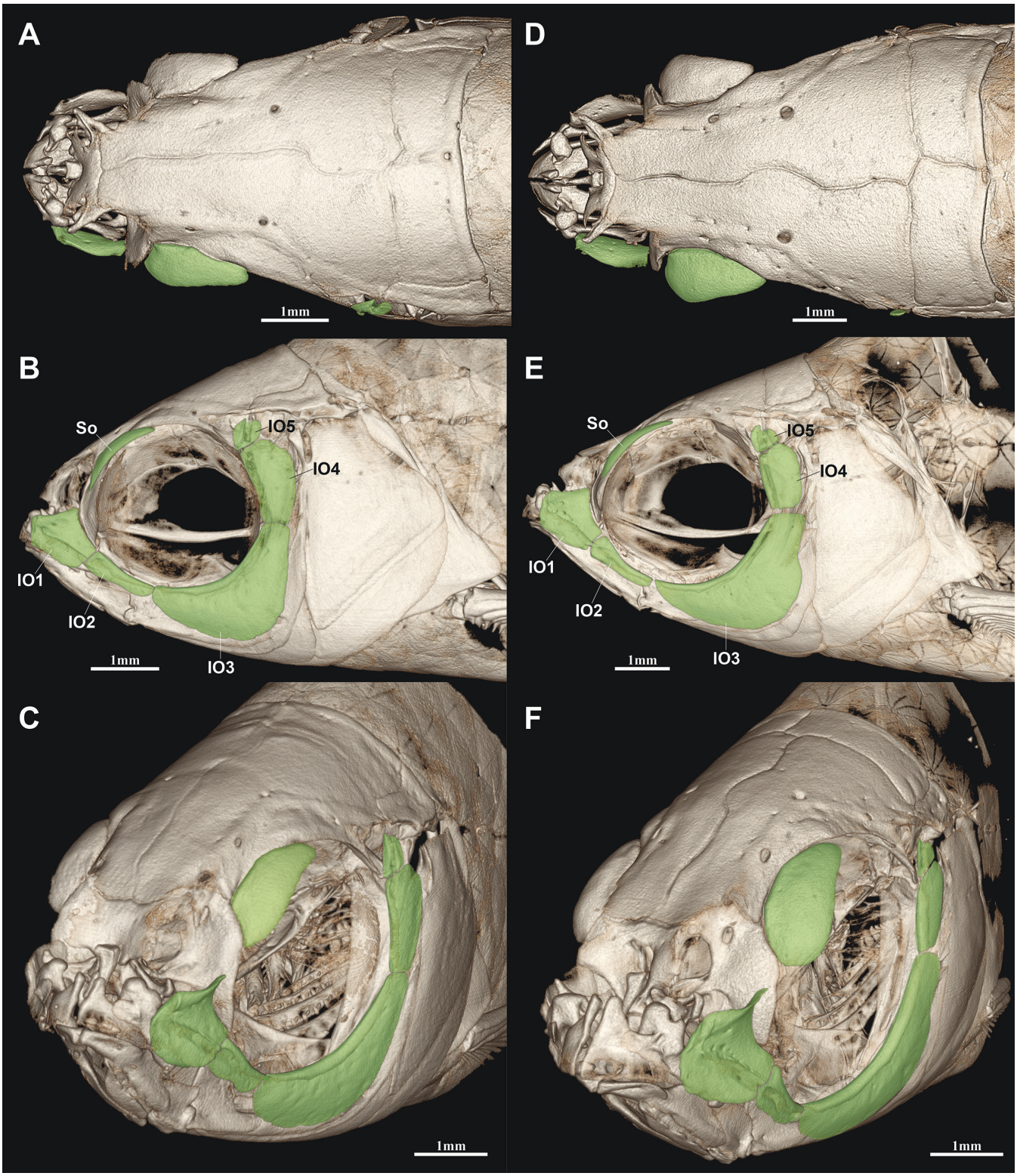

Fig. 4. CT scanned head skeleton of *Pethia* in dorsal (A, D), lateral (B, E), and anterolateral view (C, F). **A–C**, *P. castor*, TCWC 20251.01, paratype, 34.7 mm SL; **D–F**, *P. pollux,* TCWC 20250.01, paratype, 37.1 mm SL. Circumorbital bones highlighted in green. Abbreviations: IO1–5, infraorbital bones 1–5; So, supraorbital.

posterior nostril and orbit (Fig. 3C). Opaque skin overlaying a dense aggregation of connective tissue, closely associated with anterolateral extension of lateral ethmoid and dorsal edge and upper lateral face of the lachrymal (IO1).

Supraorbital well-ossified (Fig. 4A), widest anteriorly, tapering in width posteriorly, firmly attached to posterodorsal part of lateral ethmoid anteriorly. Mesethmoid irregularly shaped, weakly concave at centre (Figs. 4A, 5A), extended dorsolaterally into poorly ossified flanges of membrane bone. Skull roof complete, without post-epiphyseal fontanelle. Masticatory plate broad, oval in ventral view; centre of plate slightly concave. Pharyngeal process of basioccipital process well-developed, extending beyond imaginary vertical

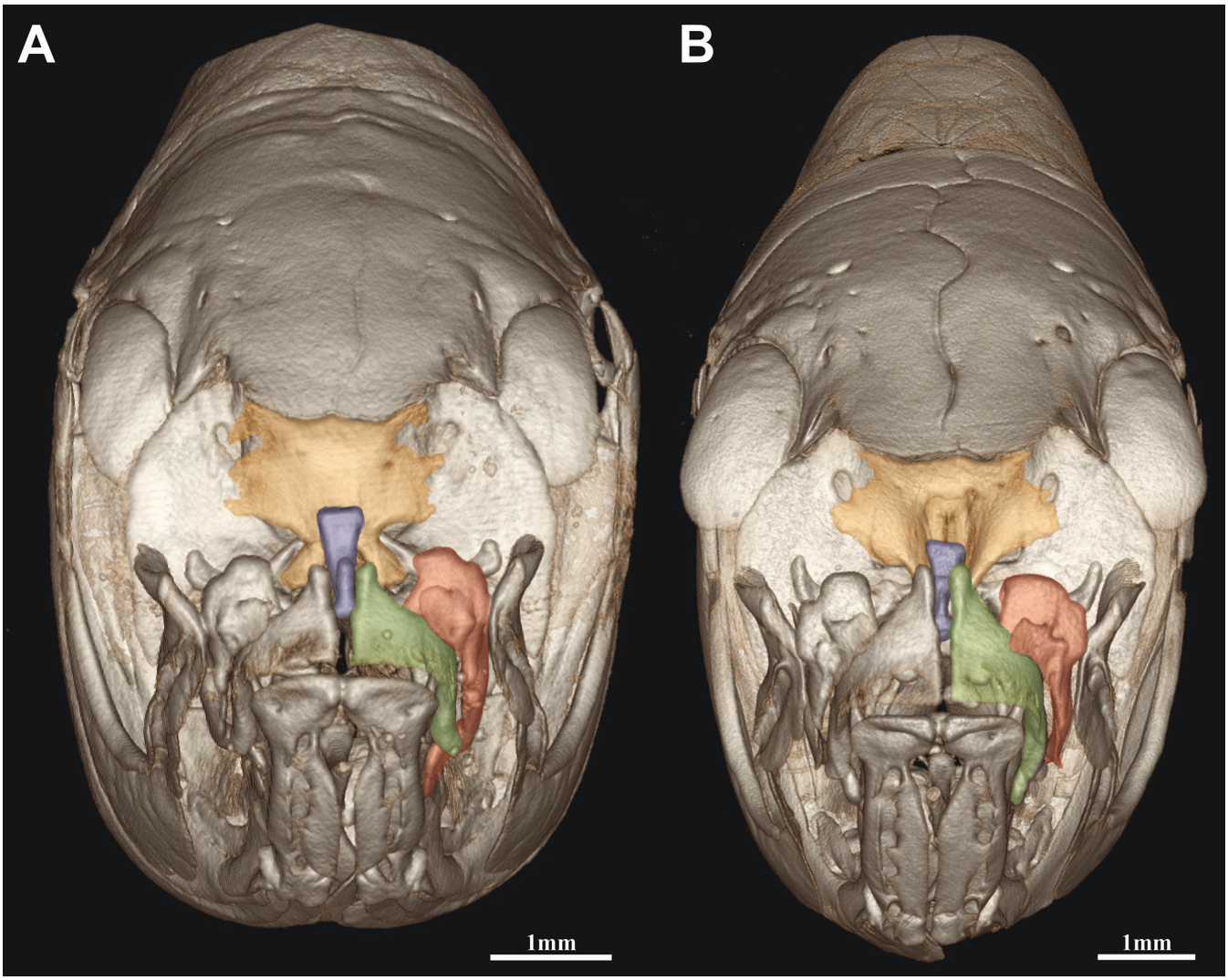

Fig. 5. CT scanned head skeleton of *Pethia* in frontal view. **A**, *P. castor*, TCWC 20251.01, paratype, 34.7 mm SL; **B**, *P. pollux*, TCWC 20250.01, paratype, 37.1 mm SL. Select bones highlighted, including: mesethmoid (light orange); kinethmoid (blue); maxilla (dark orange); premaxilla (green).

line through centre of compound centrum 2+3. General appearance of neurocranium otherwise similar to that of *P. ticto* (see Katwate et al., 2015). Ascending process of premaxilla poorly developed (Fig. 6A), terminating at point anterior to imaginary vertical line through midpoint of kinethmoid with jaws closed. Autopalatine process of maxilla and coronoid process of dentary both well-developed (Fig. 6A). Dorsal margin of angulo-articular elevated posteriorly into triangular process (Fig. 6A), overlapping ventralmost part of ectopterygoid in lateral view.

Five infraorbital bones (Fig. 4A–C); lachrymal (IO1) an irregular, shield-shaped bone, pointed dorsally, rounded anteroventrally, with poorly ossified, yet enclosed lateral line canal, with three openings located on bone, and a fourth located at junction between IO1 and IO2; IO2 narrow, with poorly ossified, yet enclosed lateral line canal, with single opening located at middle of bone, an additional pore located at junction between IO2 and IO3; IO3 broad, anterior tip at middle of orbit, anteriorly extending ventrally to middle of cheek, posteriorly extending ventrally to overlap preopercle, with open lateral-line canal; IO4 with poorly ossified, yet enclosed lateral-line canal along anterior part, without pore on bone, single pore located at junction with both IO3 and IO5; IO5 a small ossification composed largely of poorly ossified canal bone, transfers infraorbital canal to otic canal at junction between frontal and pterotic. Supraorbital lateral line canal extending from nasal, through frontal, terminating at junction with otic canal between frontal and pterotic, fully enclosed, with 6 pores, including 2 on nasal, 1 at junction between nasal and frontal, 3 along frontal dorsal to orbit, and 1 at junction between frontal and pterotic; parietal branch of supraorbital canal absent. Preoperculo-mandibular lateral line canal (Fig. 6A) starting on dentary, continuing through anguloarticular, preopercle, and opercle, terminating at junction with otic lateral line canal at centre of pterotic; fully enclosed, excluding open portion along preopercle, with 10 pores, including 3 on dentary, 1 at junction between dentary and anguloarticular, 1 at junction between anguloarticular and preopercle, 3 along preopercle, 1 at junction between preopercle and opercle, and 1 between junction of opercle and pterotic. Anterior (horizontal) part of preoperculo-mandibular lateral line canal on preopercle not fully enclosed; with roof of canal formed by skin. Otic lateral line canal

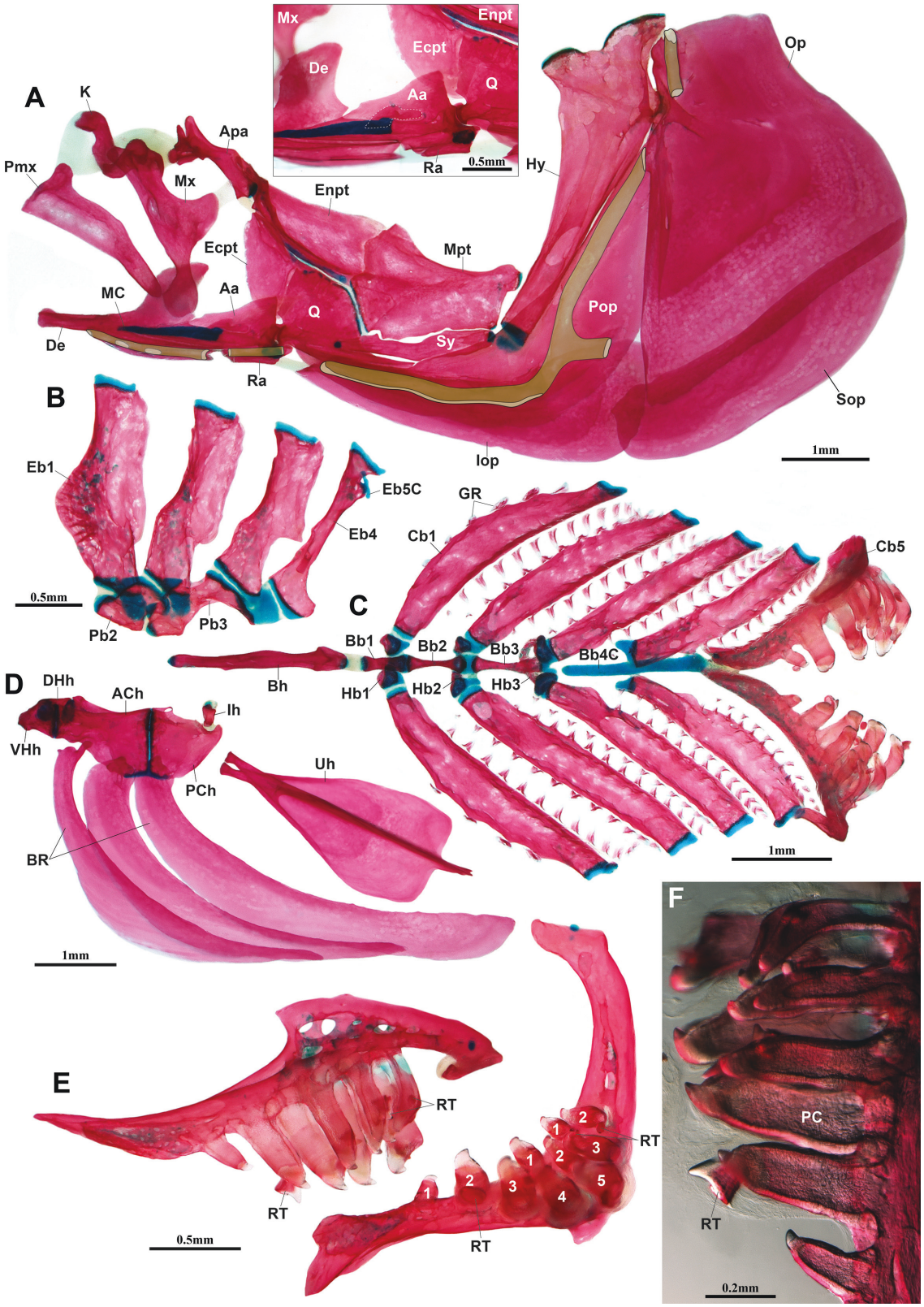

Fig. 6. Viscerocranium of *Pethia castor,* TCWC 20251.03, paratype, 38.4 mm SL. **A**, hyopalatine arch and opercular series, right side in lateral view (image reversed). Preoperculo-mandibular canal outlined in green. Inset box shows close-up of posterior part of lower jaw in medial view; **B**, dorsal gill arch elements, right side in dorsal view; **C**, ventral gill arch elements in dorsal view; **D**, hyoid bar, right side in lateral view (image reversed) and urohyal in ventral view; **E**, ceratobranchial 5, right side in oblique dorsolateral view and lateral view; **F**, close up of ceratobranchial 5 teeth, right side in dorsal view (image reversed), anterior to bottom of page. Abbreviations: Aa, anguloarticular; ACh, anterior ceratohyal; Apa, autopalatine; Bb1–3, basibranchials 1–3; Bb4C, basibranchial 4 cartilage; Bh, basihyal; BR, branchiostegal rays; Cb1–5, ceratobranchials 1–5; Cm, coronomeckelian; De, dentary; DHh, dorsal hypohyal; Eb1–4, epibranchial 1–4; Eb5C, epibranchial 5 cartilage; Ectp, ectopterygoid; Enpt, endopterygoid; Hb1–3, hypobranchials 1–3; Hy, hyomandibular; Ih, interhyal; Iop, interopercle; GR, gill raker; K, kinethmoid; MC, Meckel's cartilage; Mx, maxilla; Op, opercle; Pb2–3, pharyngobranchial 2–3; PC, pulp cavity; PCh, posterior ceratohyal; Pmx, premaxilla; Pop, preopercle; Q, quadrate; Ra, retroarticular; RT, replacement tooth; Sop, subopercle; Sy, symplectic; Uh, urohyal; VHh, ventral hypohyal.

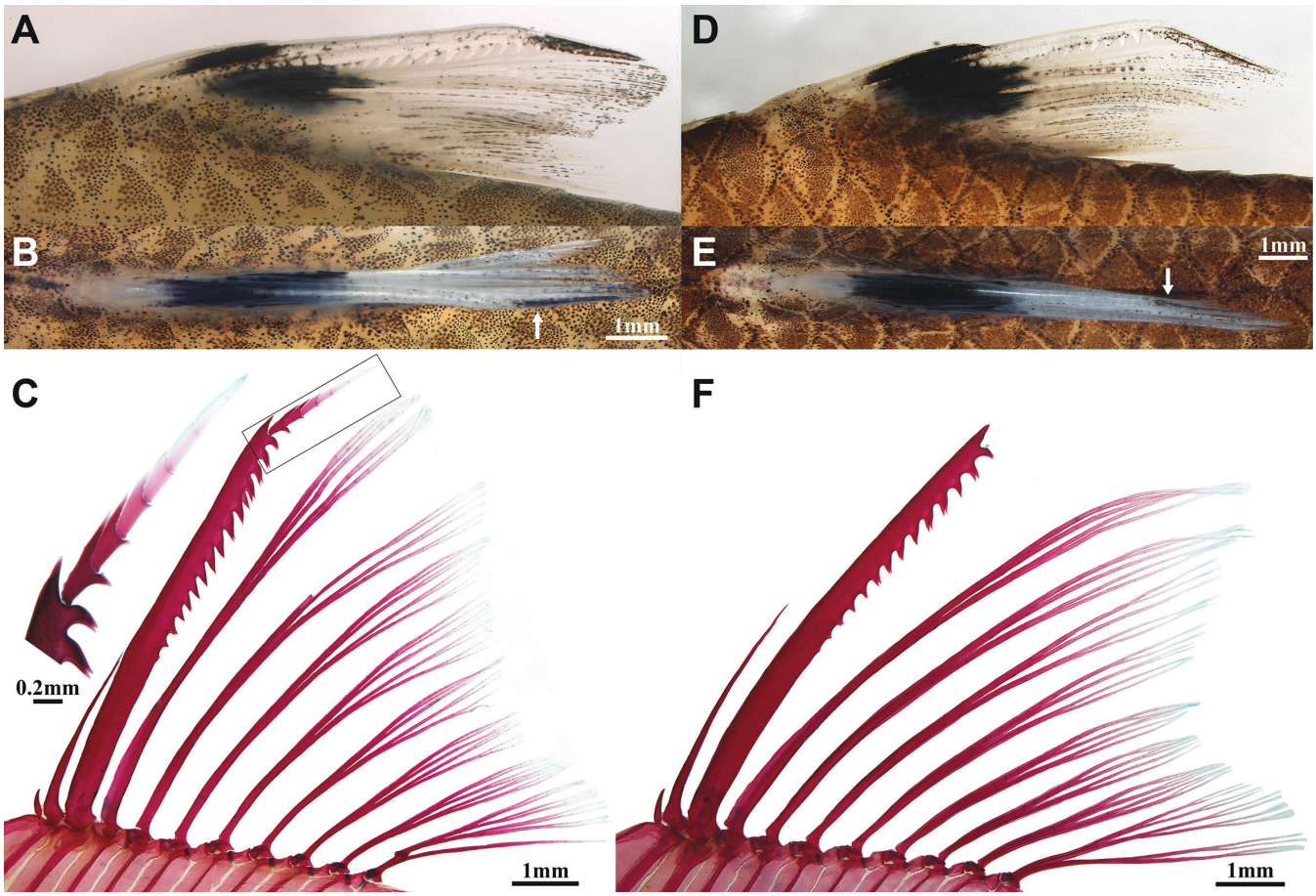

Fig. 7. Dorsal fin and skeleton of *Pethia castor* (A–C) and *P. pollux* (D–F). **A**, **B**, CMK 27085, 41.3 mm SL, in lateral (A) and dorsal (B) view; **C**, TCWC 20251.03, paratype, 38.4 mm SL, cleared and stained, inset shows close up of distal tip of last unbranched ray; **D**, **E**, CMK 28804, 35.4 mm SL, in lateral (D) and dorsal (E) view; **F**, TCWC 20250.03, paratype, 35.4 mm SL, cleared and stained. White arrow points to black pigmentation at distal tip of last unbranched ray in B and E.

located on pterotic, connecting with trunk lateral line canal via posttemporal and supracleithrum; fully enclosed with three pores, including 1 pore at junction with frontal and IO5, 1 pore at junction with opercle, and 1 pore at junction with posttemporal. Junction between supratemporal lateral line canal and otic lateral line canal located at posterior part of pterotic. Supratemporal lateral line canal with single pore close to origin; supratemporal commissure located along dorsal midline at junction of parietal bones, without pore, without contact to supraoccipital.

Gill rakers present on gill arches 1–5 (Fig. 6C), with following distribution in 2 C&S specimens: arch 1, anterior row (a) 7–8 (total), 5–6 on ceratobranchial (cb)+1 on epibranchial (eb)+1 at cb/eb junction (cej)/posterior row (p) 12–13, 9–10cb+2eb+1cej; arch 2, a14–16, 10–11cb+3–4eb+1cej/p17–18, 13–14cb+3–4eb+1cej; arch 3, a15–16, 11–12cb+3–4eb+1cej/p15–16, 11–12cb+3–4eb+1cej; arch 4, a15–16, 11–12cb+3–4eb+1cej/p12–13cb; arch 5, a13cb. Pharyngeal teeth on ceratobranchial 5 unicuspid (Fig. 6C, E, F), with slightly hooked tips, arranged in three rows, with formula 5,3,2. Epibranchial 1 with expanded, shelf-like process on anterior edge (Fig. 6B). Basihyal a thin rod. Three branchiostegal rays; tip of posteriormost ray expanded, approximately 3–4 times deeper than pointed tip of anterior rays (Fig. 6D).

Dorsal-fin rays iii.8.i (1) or iii.9 (1). Anal-fin rays iii.5.i (1) or iii.6 (1). Principal caudal-fin rays 10+9; dorsal procurrent rays 5 (1) or 6 (1), ventral procurrent rays 5 (1) or 6 (1). Pelvic-fin rays i.7.i (1) or i.8 (1). Pectoral-fin rays i.11.ii (1) or i.12 (1). Dorsal-fin origin slightly anterior to pelvic-fin origin; posterior margin slightly concave. Last unbranched ray almost as long as first branched ray; proximal ⅔ compact, approximately twice as thick as first branched ray, rigid, strongly serrated, with 14–15 pairs of serrae on distal ⅔; apical ⅓ flexible, segmented, without serrae, or with poorly developed serrae on one or two proximal segments (Fig. 7C). Anal-fin origin posterior to vertical through base of posterior dorsal-fin ray; posterior margin slightly concave. Caudal fin deeply emarginate; tip of lobes rounded. Pelvic-fin tip rounded to weakly pointed, adpressed fin reaching to vent. Pectoral-fin tip rounded, adpressed fin reaching one scale row anterior to pelvic-fin origin.

Body lateral line incomplete, continuous for 9 (1), 10 (2), 11 (3*), 12 (1), 14 (2) or 16 (1) scales. Lateral line gently curved, lowest point located on 7th or 8th scale. Scales in lateral line scale row 22 (4) or 23 (5*), plus 1 (3) or 2 (4*) on base of caudal fin. Predorsal scales 7 (1) or 8 (10*). Circumpeduncular scales 12 (½/5/½). Scales in transverse row starting at dorsal-fin origin ½4/1/2½. 4–5 well-developed radii on anterior and posterior field of each scale. Pseudotympanum located

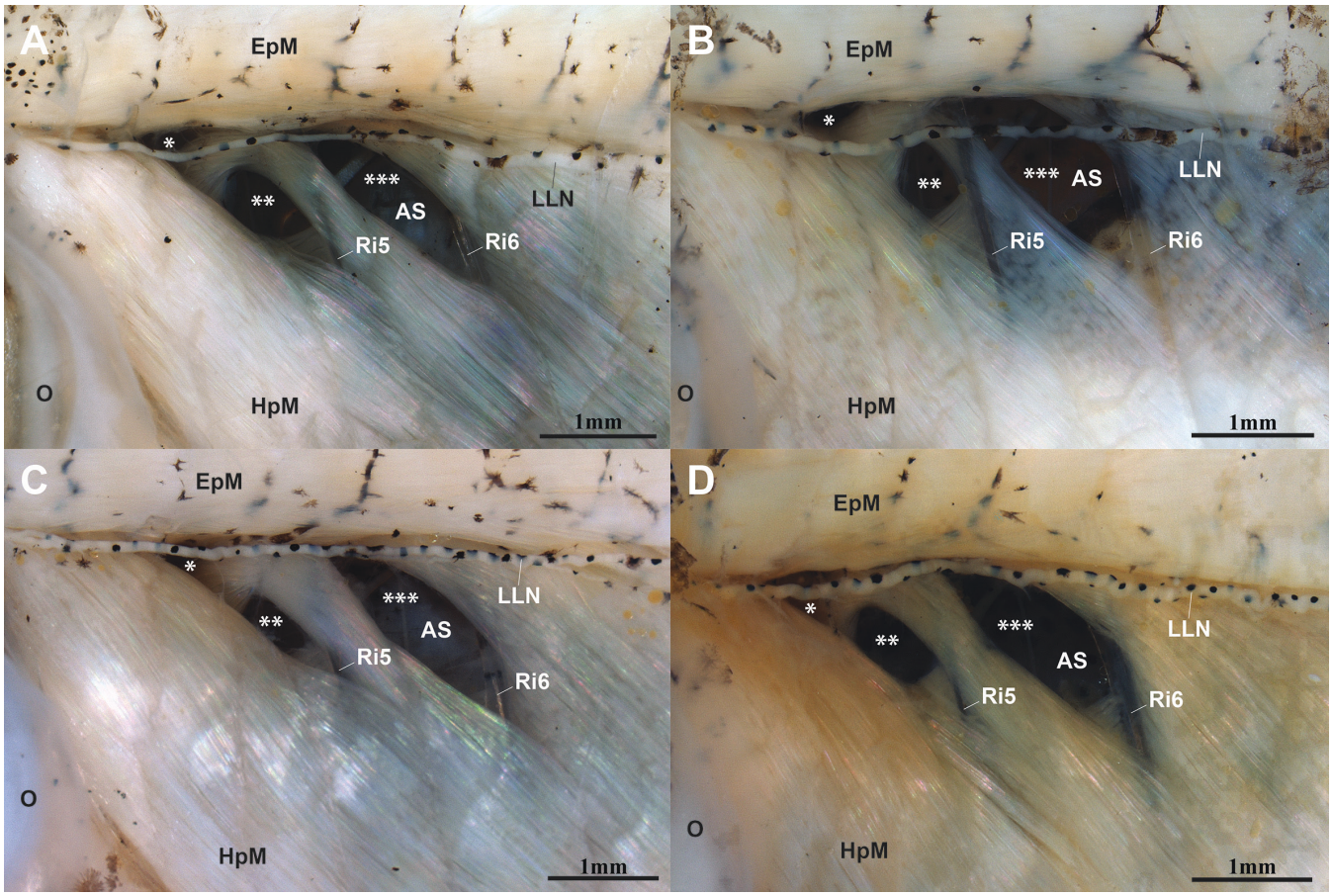

Fig. 8. Pseudotympanum of *Pethia castor* (A, B) and *P. pollux* (C, D). **A**, *P. castor*, 20251.02, paratype, male, 35.2 mm SL; **B**, *P. castor*, TCWC 20251.02, paratype, female, 36.2 mm SL; **C**, *P. pollux,* TCWC 20250.02, paratype, male, 35.8 mm SL; **D**, *P. pollux,* TCWC 20250.02, paratype, female, 38.2 mm SL. Overlying scales and skin removed. Asterisks (*, **, ***) indicate openings in body musculature. Abbreviations: AS, anterior swimbladder chamber; EpM, epaxial musculature; HpM, hypaxial musculature; LLN, lateral line nerve; O, operculum; Ri5–6, ribs 5–6.

beneath third and fourth scales in lateral line row (Fig. 8A, B), comprising three openings in hypaxial body musculature; two small, round openings located anterior to 5th rib, larger elongate opening located between 5th and 6th ribs, through which anterior swimbladder chamber is visible. Myosepta anterior to pseudotympanum; musculature associated with 5th and 6th rib more pronounced in male (Fig. 8A) than in female (Fig. 8B).

Total number of vertebrae 30, with 16 abdominal+14 caudal. Total number of ribs 12, on vertebrae 5–16. First dorsal-fin pterygiophore inserted between neural spines of vertebrae 8/9. First anal-fin pterygiophore inserted between hemal spines of vertebrae 17/18. Free supraneurals 3, well developed, inserted between neural spines of vertebrae 4/5, 6/7, 8/9. Outer arm of os suspensorium elongate, reaching past imaginary horizontal line through dorsalmost tip of postcleithrum. Six hypurals in caudal skeleton. Free uroneural (second) absent.

Colouration. In formalin, about 1 month after fixation (Fig. 1A, B). Body background colour yellowish to light cream. Dorsal half of body (above horizontal septum) light brown, caused by pigmentation on scales (see below). Indistinct blackish-grey horizontal stripe along side of body, in deeper layer dorsal to thin black axial streak along horizontal septum; most distinct along posterior half of body in males. Scales above horizontal septum with dense scattering of light brown melanophores over much of scale pockets; a thin row of light brown melanophores bordering posterior margin of each scale, separated from anterior melanophores by crescentic unpigmented area. Melanophores on scales contributing to weak reticulate pattern on dorsal surface of body. Scales below horizontal septum with little pigment, restricted to sparse scattering of small faint brown melanophores on scale pocket and slightly darker brown melanophores along posterior edge, most obvious on scales covering pseudotympanum and lower part of caudal peduncle after some time in alcohol (Figs. 1C, D, 2A). Dorsal surface of head and lateral surface of snout with dense scattering of dark brown melanophores (Fig. 3). Sparse scattering of dark brown melanophores on skin covering upper part of opercle and around ventral margin of orbit (Fig. 3). Dorsal fin with two black markings on anterior half (Fig. 7A, B), including a larger marking over base of second unbranched to third branched ray and intervening fin membranes, and a smaller marking covering distal, flexible tip of third unbranched ray. Dorsal fin with sparse scattering of light brown melanophores distally, most evident along branched tips of rays. Centre of dorsal fin with a faint triangular canary-yellow marking in specimens after 1 month in formalin (Fig.

Fig. 9. Map of Myanmar showing localities from which specimens of *Pethia castor* and *P. pollux* were collected. Black circles, *P. castor*; white circles, *P. pollux*; grey symbols, both species. Triangle represents type locality of *P. castor*. Square represents type locality of *P pollux*.

1A, B), and possibly also in life; absent in alcohol-preserved specimens in which dorsal fin, other than black markings, is hyaline (Fig. 1C, D). Caudal fin with faint canary yellow in formalin-fixed material, hyaline in alcohol, except for light scattering of light brown melanophores over base of upper- and lowermost principal caudal-fin rays. Pectoral fin hyaline, except for sparse scattering of dark brown to black melanophores over four anteriormost rays; melanophores associated with anteriormost pectoral-fin ray darker than on other rays, creating faint black to dark brown stripe, better developed in males. Pelvic fin and anal fin hyaline. Colour in life not recorded.

Sexual dimorphism. No obvious external sexual dimorphism other than slight dichromatism described above under section on colouration. Minute conical tubercles scattered over dorsal surface of head in two male specimens (CMK 27085). Hypaxial musculature surrounding pseudotympanum slightly hypertrophied in male, most obvious in hypaxial myomeres anterior to structure and hypaxial musculature surrounding 5th and 6th rib. Mature females with swollen abdomens; ripe ovaries visible through body side in preserved specimens,

Fig. 10. Ayeyarwady River plain. **A**, backwaters of Ayeyarwady River upstream of Hti Chaint (Sagaing Region), habitat of *Pethia castor* (CMK 27144); **B**, ponded stream near floodplain lake near Shwegu (Kachin State, Myanmar), habitat of both *P. castor* (CMK 28806) and *P. pollux* (CMK 27070; type locality).

light cream in colour. One dissected female with ripe ovary containing ~200 eggs of diameter 0.6–0.8 mm.

Distribution. Known to date only from a few sites in the middle Ayeyarwady (Fig. 9), between Bhamo and Mandalay. The majority of specimens were collected from the type locality, at the mouth of outlet of Indaw Inn into Ayeyarwady River. At the time of collection (June–July, beginning of floods) all sampling sites were along edges of floodplain lakes, backwaters and the Ayeyarwady proper, with murky water and mud bottom. At three sites, *P. castor* and *P. pollux* were collected together. The species were not identified in the field and no habitat preference could be noted. At two sites, *P. castor* was more abundant (Fig. 10A), and at the third site (Fig. 10B) *P. pollux* was more abundant. At the time of collection, this last site was a small ponded stream, separated from a lake, but which floods would soon connect; the stream was flowing from an area shaded by trees and bushes and the water was slightly clearer. This suggests that *P. pollux* might prefer clearer water and shade.

Etymology. Castor, the mortal twin half-brother of Pollux in Greek mythology, who gave the name of a star of the constellation and astrological sign of Gemini (twins). A noun in apposition.

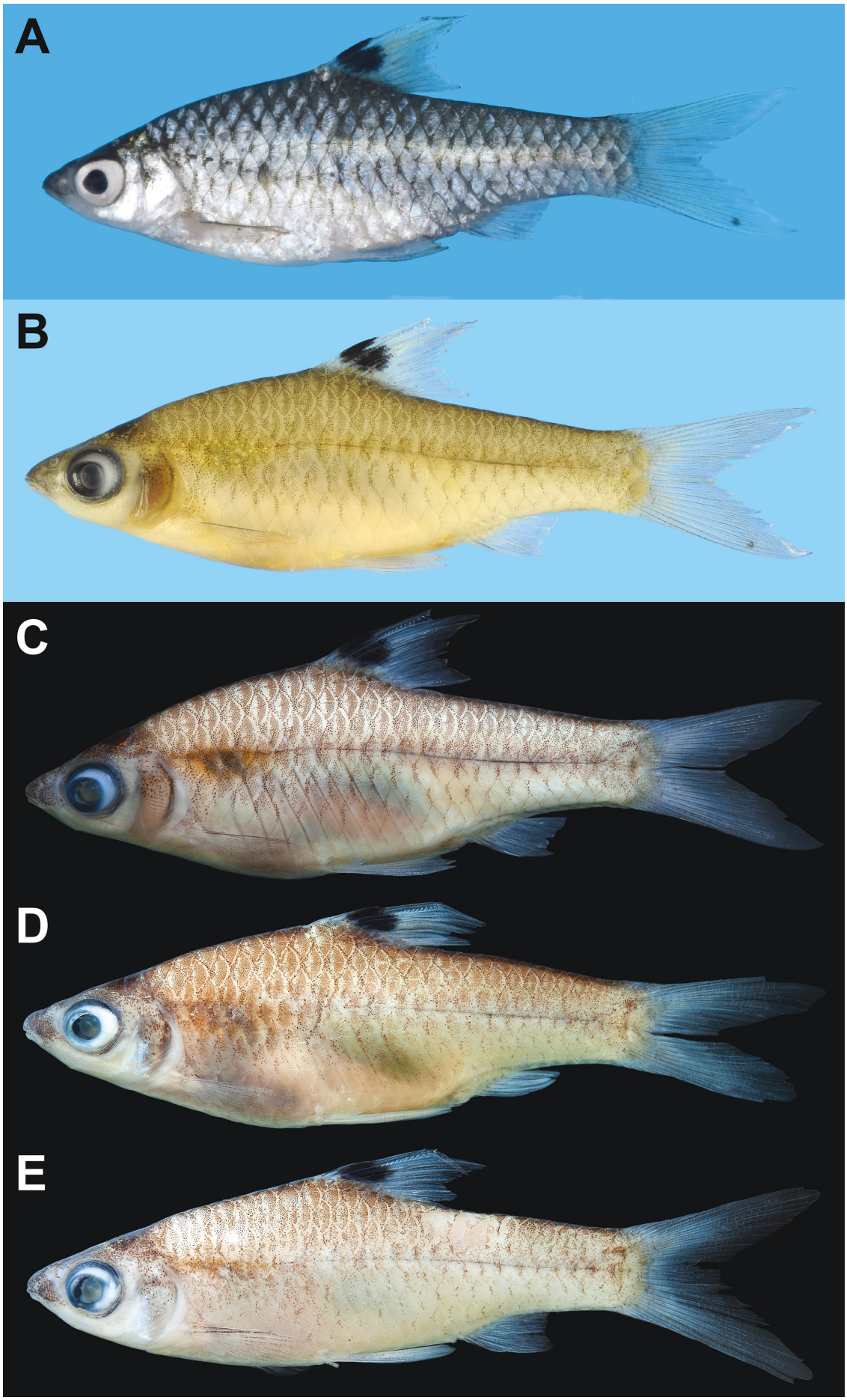

Fig. 11. *Pethia pollux*, Myanmar, Kachin State. **A–C**, MHNG 2785.034, holotype, female, 40.4 mm SL (right side, images reversed); **D**, CMK 28804, paratype, female, 41.3 mm SL; **E**, CMK 28804, paratype, male, 33.2 mm SL.

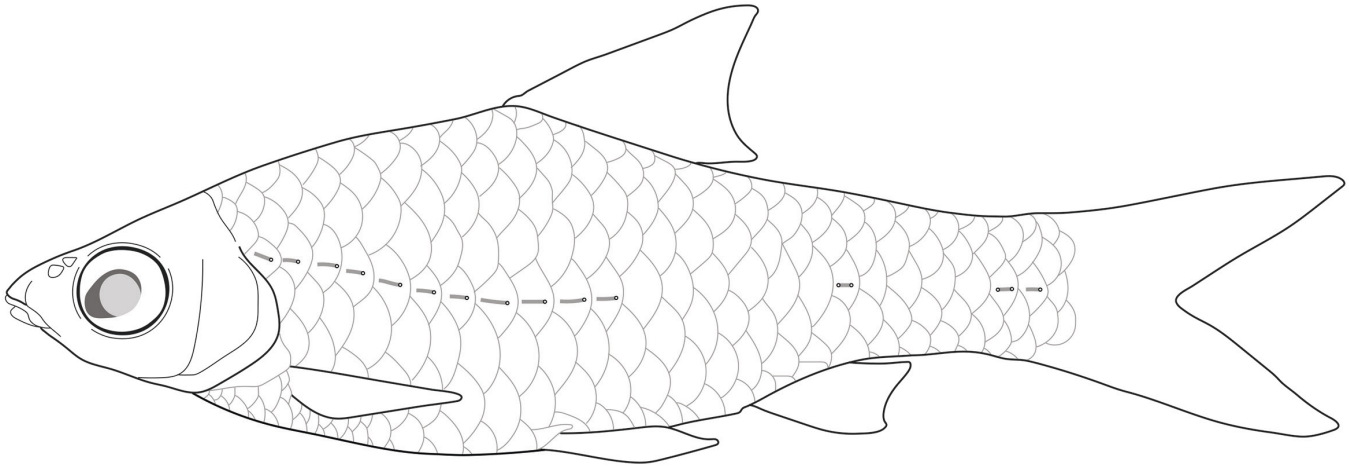

Fig. 12. Schematic diagram of *Pethia pollux* illustrating lateral line canal on body.

***Pethia pollux*, new species**
(Fig. 11)

Holotype. MHNG 2785.034, 40.4 mm SL; Myanmar: Kachin State: Tan Pway Kone Chaung at northern edge of Thila Pha Inn, Indaw Inn, 24°18′15″N 96°48′42″E [near Shwegu]; M. Kottelat & Nyein Chan, 27 June 2017.

Paratypes. All Myanmar. **Kachin State:** CMK 27070, 3, 36.1–39.3 mm SL; 2, 38.2–40.9 mm SL [DNA voucher, fixed in 95% ethanol]; same as holotype. — CMK 28804, 12, 38.6–43.2 mm SL; ZRC 61663, 5, 36.3–39.9 mm SL; TCWC 20250.01, 1 [CT voucher, M87992], 37.1 mm SL; TCWC 20250.02, 4, 35.8–41.7 mm SL; TCWC 20250.03, 3 [C&S], 35.4 –40.0 mm SL; mouth of outlet of Indaw Inn into Ayeyarwady River, 24°13′08″N 96°49′25″E [near Shwegu]; M. Kottelat & Nyein Chan, 27 June 2017.

Sagaing Region: CMK 28807, 2, 26.1–28.3 mm SL; Ayeyarwady River near Hti Chaint Myit Yoe, 23°43′59″N 96°09′50″E; M. Kottelat & Nyein Chan, 30 June 2017. — CMK 27937, 1, 39.3 mm SL [DNA voucher, fixed in 95% ethanol]; Ayeyarwady River near Hti Kone village, about 55 km North of Mandalay, 22°26′41″N 96°00′18″E; M. Kottelat et al., 2 July 2017.

Additional material (non-types)**.** CMK 28805, 56, 33.6–41.6; Myanmar: Kachin State: mouth of outlet of Indaw Inn into Ayeyarwady River, 24°13′08″N 96°49′25″E; M. Kottelat & Nyein Chan, 27 June 2017. — UF 191631, 10 [2 C&S], 29.8–35.8 mm SL; Myanmar: Kachin State: Ayeyarwady drainage, Bhamo Market (24°15′00″N 97°12′36″E), purchased from fishermen by T. R. Roberts, April 2002. — CMK 26822, 2, 26.4–33.8 mm SL; Myanmar: Sagaing Region: oxbow lake of Ayeyarwady River, about 37 km downriver of Shwegu, 92 masl, 24°17′11″N 96°28′30″E; Nyein Chan, 9 February 2017.

Diagnosis. *Pethia pollux* is distinguished from all congeners, except *P. castor*, by the absence of black blotches (round or vertically elongate) on the body and by the presence of two black markings on anterior half of dorsal fin, including a larger marking over base of second unbranched to third branched ray and intervening fin membranes, and a smaller marking covering distal, flexible tip of third unbranched ray.

The external differences in preserved material of *P. pollux* and *P. castor* are not striking and may not be discernible in not optimally preserved specimens. *Pethia pollux* is distinguished from *P. castor* by: lacking a horizontal stripe along body side (vs. a weak stripe present, most evident in males); scales located on lower half of caudal peduncle, with dense scattering of dark brown melanophores, forming distinct reticulate pattern (Fig. 2B; vs. with few faint brown melanophores forming weak or barely discernible reticulate pattern); presence of isolated lateral-line canal ossicles on scales in lateral line canal row on posterior part of body (Fig. 12; vs. absence); a slightly larger eye (orbit diameter 32–36% HL vs. 29–33); a slightly longer (23–29% HL vs. 19–25), more pointed (vs. rounded) snout; upper lip swollen posteriorly (vs. upper lip uniform thickness along lateral margin of jaw); lateral fold on snout well developed (vs. poorly developed) along anterior margin of lachrymal; rostral cap swollen, obvious in lateral view, overlapping upper lip at midline (vs. rostral cap barely discernible from remainder of snout, not overlapping upper lip dorsally).

The following osteological characters too, distinguish *P. pollux* from *P. castor*: ascending process of premaxilla moderately developed, posteriormost tip reaching past midpoint of kinethmoid when jaws closed (vs. poorly developed, posteriormost tip not reaching to midpoint of kinethmoid when jaws closed); posterior part of anguloarticular with flat dorsal margin (vs. posterior part of anguloarticular elevated dorsally as large triangular process); central part of mesethmoid with cavernous indentation (vs. weakly concave); supraorbital relatively wide anteriorly, tapering in width abruptly towards posterior, without contact to lateral ethmoid (vs. relatively narrow anteriorly, tapering in width gently towards posterior, firmly attached to lateral ethmoid anteriorly); anterior edge of epibranchial 1 with poorly developed (vs. well-developed), shelf-like anterior extension.

Description. See Figure 11 for general appearance and Table 1 for morphometric data obtained from holotype and

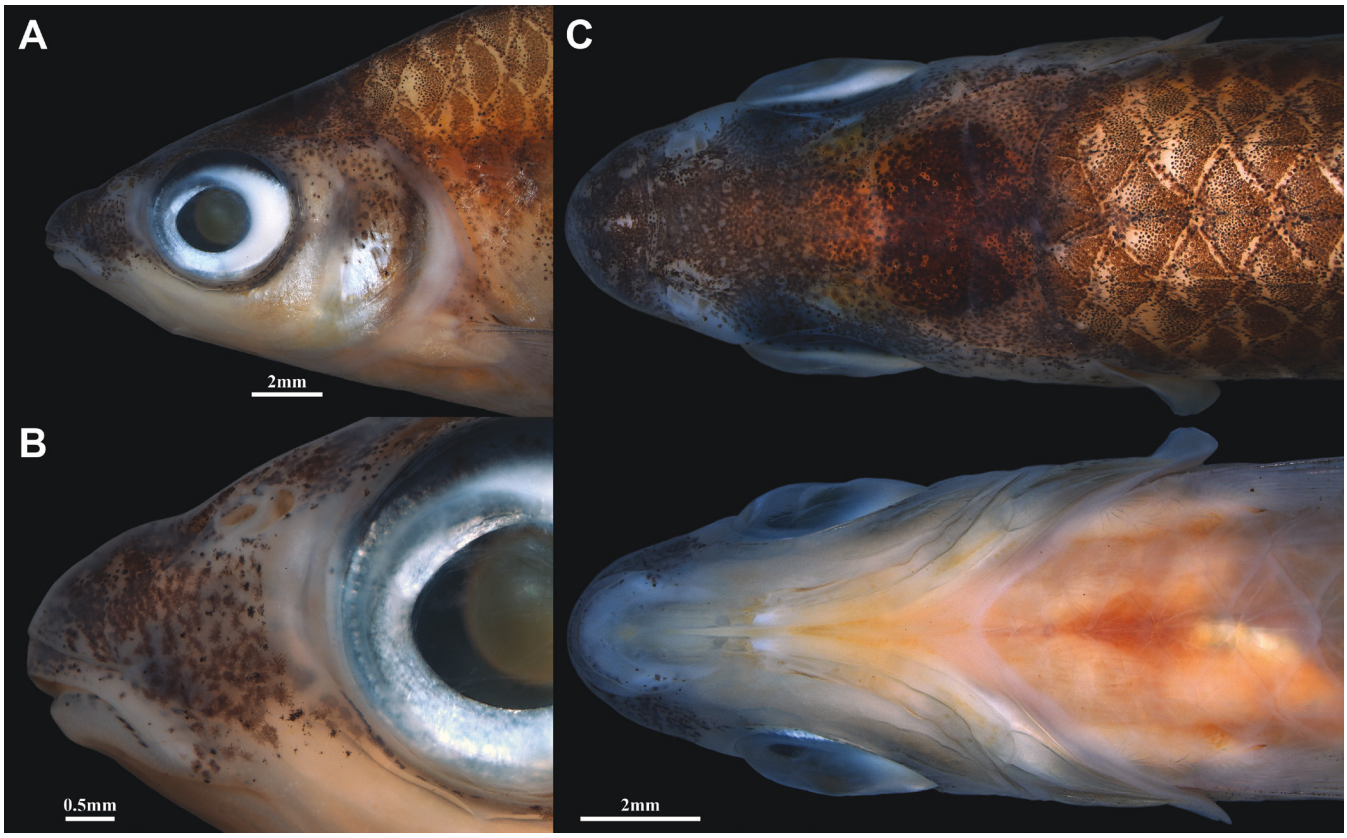

Fig. 13. *Pethia pollux*, CMK 28804, 41.3 mm SL. **A**, head in lateral view; **B**, close up of snout in lateral view; **C**, head in dorsal and ventral view.

9 paratypes. Body laterally compressed, relatively deep, greatest depth at dorsal-fin origin. Caudal peduncle depth approximately equal to head depth through orbit. Dorsal profile continuous between head and body, with slight hump at nape; ascending, almost straight, prior to dorsal fin, descending, almost straight, from dorsal-fin origin to just anterior of base of caudal fin, slightly concave at base of caudal fin. Ventral profile of head and body continuous, rounded through pelvic- and anal-fin base, slightly concave along caudal peduncle.

Head short, laterally compressed (Fig. 13). Orbit diameter greater than snout length. Pupil oval, with apex located within anteroventral part of eye in lateral view (Fig. 13A, B). Snout moderately pointed. Mouth small, subterminal, reaching vertical line through anterior margin of anterior nostril. Lips exposed, smooth, moderately thick; lower lip fold interrupted medially; upper lip slightly expanded posteriorly, starting at point opposite lateral fold on snout. Lateral fold on snout located along anterior margin of lachrymal (IO1), well-developed, continuous with shallow groove over dorsal surface of snout. Rostral cap conspicuous, visible in lateral view as swelling at anterior tip of snout; anteriormost part of rostral cap overlapping dorsal part of upper lip along midline (Fig. 13B). Barbels absent. Skin anterior to eye thick, depigmented, opaque (Fig. 13B), visible in dorsal view as a clear, slightly bulbous patch of skin between posterior nostril and orbit (Fig. 13C). Opaque skin overlaying a dense aggregation of connective tissue, closely associated with anterolateral extension of lateral ethmoid and dorsal edge and upper lateral face of the lachrymal (IO1).

Supraorbital well-ossified (Fig. 4D), widest at point approximately ⅓ from anterior tip, tapering in width abruptly towards posterior; separate from lateral ethmoid anteriorly. Mesethmoid irregularly shaped; centre with cavernous indentation (Figs. 4F, 5B), extended dorsolaterally into poorly ossified flanges of membrane bone. Skull roof complete, without post-epiphyseal fontanelle. Masticatory plate broad, oval in ventral view; centre of plate slightly concave. Pharyngeal process of basioccipital process well-developed, extending beyond vertical through centre of compound centrum 2+3. General appearance of neurocranium otherwise similar to that of *P. ticto* (see Katwate et al., 2015). Ascending process of premaxilla moderately developed (Fig. 14A), terminating at point posterior to imaginary vertical line through midpoint of kinethmoid with jaws closed. Autopalatine process of maxilla and coronoid process of dentary both well developed (Fig. 14A). Dorsal margin of posterior part of anguloarticular horizontal (Fig. 14A).

Cephalic lateral line canal system as described for *P. castor*, except preoperculo-mandibular lateral line canal open (roof formed by skin only) along entire horizontal part of preopercle (Fig. 14A).

Gill rakers present on gill arches 1–5 (Fig. 14C), with following distribution in 3 C&S specimens: arch 1, a7, 5cb+1eb+1cej/p13–14, 10–11cb+2eb+1cej; arch 2, a13–15, 9–10cb+3–4eb+1cej/p14–16, 10–11cb+3–4eb+1cej; arch 3, a14–16, 10–11cb+3–4eb+1cej/p15–16, 11–12cb+3–4eb+1cej; arch 4, a15–16, 11cb+3–4eb+1cej/p11–12cb; arch 5, a10–11cb. Pharyngeal teeth on ceratobranchial 5 unicuspid,

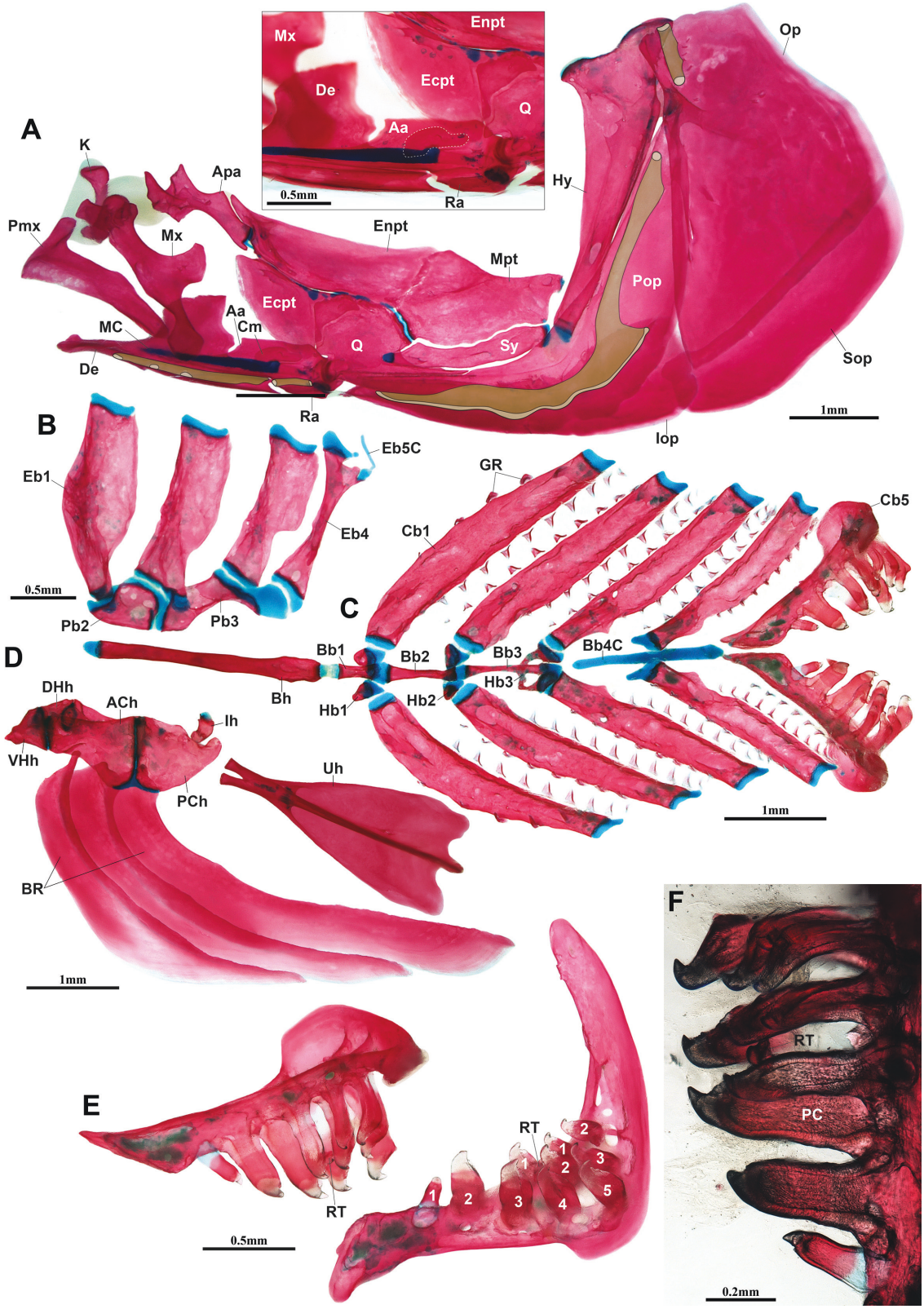

Fig. 14. Viscerocranium of *Pethia pollux*, TCWC 20250.03, paratype, 35.4 mm SL. **A**, hyopalatine arch and opercular series, right side in lateral view (image reversed). Preoperculo-mandibular canal outlined in green. Inset box shows close-up of posterior part of lower jaw in medial view; **B**, dorsal gill arch elements, right side in dorsal view; **C**, ventral gill arch elements in dorsal view; **D**, hyoid bar, right side in lateral view (image reversed) and urohyal in ventral view; **E**, ceratobranchial 5, right side in oblique dorsolateral view and lateral view; **F**, close up of ceratobranchial 5 teeth, right side in dorsal view (image reversed), anterior to bottom of page. Abbreviations: Aa, anguloarticular; ACh, anterior ceratohyal; Apa, autopalatine; Bb1–3, basibranchials 1–3; Bb4C, basibranchial 4 cartilage; Bh, basihyal; BR, branchiostegal rays; Cb1–5, ceratobranchials 1–5; Cm, coronomeckelian; De, dentary; DHh, dorsal hypohyal; Eb1–4, epibranchial 1–4; Eb5C, epibranchial 5 cartilage; Ectp, ectopterygoid; Enpt, endopterygoid; Hb1–3, hypobranchials 1–3; Hy, hyomandibular; Ih, interhyal; Iop, interopercle; GR, gill raker; K, kinethmoid; MC, Meckel's cartilage; Mx, maxilla; Op, opercle; Pb2–3, pharyngobranchial 2–3; PC, pulp cavity; PCh, posterior ceratohyal; Pmx, premaxilla; Pop, preopercle; Q, quadrate; Ra, retroarticular; RT, replacement tooth; Sop, subopercle; Sy, symplectic; Uh, urohyal; VHh, ventral hypohyal.

arranged in three rows, with formula 5,3,2 (Fig. 14C, E, F); tip of crown strongly hooked with weakly serrated surface medial to hooked portion visible on some teeth (Fig. 14F). Anterior edge of epibranchial 1 weakly convex (Fig. 14B). Three branchiostegal rays; tip of posteriormost ray expanded, approximately 3–4 times deeper than pointed tip of anterior rays (Fig. 14D).

Dorsal-fin rays iii.8.i (3) or iii.9 (2). Anal-fin rays iii.5.i (3) or iii.6 (2). Principal caudal-fin rays 10+9; dorsal procurrent rays 6 (4) or 7 (1), ventral procurrent rays 5 (4) or 6 (1). Pelvic-fin rays i.7.i (2), i.8 (1) or i.8.i (2). Pectoral-fin rays i.10.i (1), i.11.i (2), i.11.ii (1) or i.12 (1). Dorsal-fin origin slightly anterior to pelvic-fin origin; posterior margin slightly concave. Last unbranched ray almost as long as first branched ray (Fig. 7F); proximal ⅔ compact, approximately twice as thick as first branched ray, rigid, strongly serrated, with 14–15 pairs of serrae on distal ⅔; apical ⅓ flexible, segmented, without serrae, or with poorly developed serrae on one or two proximal segments; apical ⅓ of ray (developing portion) fragile, missing from majority of specimens (including preserved holotype, but present at time of capture; Fig. 11A). Anal-fin origin posterior to vertical through base of posteriormost dorsal-fin ray; posterior margin straight to slightly concave. Caudal fin deeply emarginate; tip of lobes weakly pointed. Pelvic-fin tip pointed, adpressed fin reaching vent. Pectoral-fin tip rounded, adpressed fin reaching one scale row anterior to pelvic-fin origin.

Body lateral line incomplete, continuous for 8 (1), 9 (3), 10 (1), 11 (1*), 12 (1), 13 (1), 14 (1) or 16 (1) scales, followed in majority of specimens by several (most commonly 1–2, up to 5) isolated lateral line canal ossicles on scales in lateral line row along caudal peduncle (Fig. 12). Lateral line gently curved, lowest point located on 7th or 8th scale. Scales in lateral-line scale row 23 (4) or 24 (5*), plus 1 (4) or 2 (5*) on base of caudal fin. Predorsal scales 8. Circumpeduncular scales 12 (½/5/½). Scales in transverse row starting at dorsal-fin origin ½4/1/2½. Four to five well-developed radii on anterior and posterior field of each scale. Pseudotympanum located beneath third and fourth scales in lateral-line row (Fig. 8C, D), comprising three openings in hypaxial body musculature; two small, round openings located anterior to 5th rib, larger elongate opening located between 5th and 6th rib through which anterior swimbladder chamber is visible. Myosepta anterior to pseudotympanum; musculature associated with 5th rib more pronounced in male (Fig. 8C) than in female (Fig. 8D).

Total number of vertebrae 30, with 16 abdominal+14 caudal. Total number of ribs 12, on vertebrae 5–16. First dorsal-fin pterygiophore inserted between neural spines of vertebrae 8/9 (4) or 9/10 (1). First anal-fin pterygiophore inserted between hemal spines of vertebrae 17/18 (4) or 18/10 (1). Free supraneurals 3, well developed, inserted between neural spines of vertebrae 4/5, 6/7, 8/9. Outer arm of os suspensorium elongate, reaching past imaginary horizontal line through dorsalmost tip of postcleithrum. 6 hypurals in caudal skeleton. Free uroneural (second) absent.

Colouration. In formalin, about 1 month after fixation (Fig. 11B). Body background colour yellowish to light cream. Scales (excluding those of lowermost abdomen) with variable brown pigment (see below). Thin black axial streak along horizontal septum, most evident on posterior ⅔ of body, obscured by scale pigment anteriorly. Scales above horizontal septum generally with dense scattering of light brown melanophores over most of scale surface, excluding an anterior depigmented area posterior to anterior scale base and a posterior, crescent-shaped depigmented area close to posterior margin. Scales below horizontal septum (excluding those on lower abdomen) with cluster of dark brown melanophores on scale pocket, forming a regular pattern of small vertically elongate markings, most obvious on lateral line canal bearing scales and those scales in row immediately below, indistinct on lower part of caudal peduncle. Scales on lower half of caudal peduncle with single row of brown melanophores along posterior margin, creating weak reticulate pattern (Fig. 2B). Dorsal surface of head and lateral surface of snout with dense scattering of dark brown melanophores (Fig. 13). Sparse scattering of dark brown melanophores on skin covering upper part of opercle and around ventral margin of orbit (Fig. 13A). Dorsal fin with two black markings on anterior half (Fig. 7D, E), including a larger marking over base of second unbranched to third branched ray and intervening fin membranes, and a smaller, indistinct marking covering distal, flexible tip of third unbranched ray. Dorsal fin with light scattering of brown or black melanophores distally, most obvious along branched tips of rays. Caudal fin hyaline in alcohol, except for light scattering of brown melanophores over base of upper- and lowermost principal caudal-fin rays. Anal fin with light scattering of brown melanophores, most obvious over branched tips of rays. Pectoral fin hyaline, except for light scattering of dark brown to black melanophores over four anteriormost rays; melanophores associated with anteriormost pectoral-fin ray darker than on other rays, creating faint black to dark brown stripe, better developed in males. Pelvic fin hyaline.

In life. Upper part of body and caudal peduncle blueish-silver (Fig.11A). Abdominal region silvery. Infraorbital and opercular bones with large amounts of guanine and reflective, appearing silvery. Larger marking over anterior dorsal-fin base black. Smaller marking at tip of dorsal fin and markings on other fins indistinct.

Sexual dimorphism. No obvious external sexual dimorphism. Hypaxial musculature surrounding pseudotympanum slightly hypertrophied in male, most obvious in hypaxial myomeres anterior to structure and hypaxial musculature surrounding 5th rib. Mature females with swollen abdomens; ripe ovaries visible through body side in preserved specimens, light cream in colour. One dissected female with ripe ovary containing ~250 eggs of diameter 0.6–0.8 mm.

Distribution. Known to date from only a few sites in the middle Ayeyarwady (Fig. 9), between Bhamo and Mandalay. The type locality, Tan Pway Kone Chaung at northern edge of Thila Pha Inn, was a pond in a very slow-flowing stream

at the edge of the floodplain (Fig. 10B), with moderately clear water (as compared to the murky adjacent marsh and lake). Numerous submerged aquatic plants were present (in contrast to the adjacent flooded lakes). See under *P. castor* for more information.

Etymology. Pollux, divine twin half-brother of Castor in Greek mythology, alluded also in the name of a star of the constellation and astrological sign of Gemini (twins). A noun in apposition.

Genetic Distances. The mean genetic distance (uncorrected *p*-distance) between the COI sequences obtained for *P. pollux* (n=3; see Appendix 1 for GenBank numbers and museum voucher numbers) differed by 0.1% (range 0–0.1%). Sequences obtained for *P. pollux* differed from those of *P. castor* (n=2) by 8.2%.

DISCUSSION

Pethia castor and *P. pollux* are externally similar, and material representing the two species was not distinguished during field sampling. This may be partly explained by the bleached pattern typical of fish in murky water. Also, the largest series (CMK 27085, 28787, 28804, 28805) were obtained from traps and the fish were already dead and, in some cases, damaged. Examination of the samples revealed subtle differences in snout shape and body pigmentation, later corroborated by the examination of cleared and stained specimens. Though the morphological differences between *P. castor* and *P. pollux* are subtle (see diagnoses), the genetic distance between the two species based on COI sequences obtained from paratypes (see Appendix 1) is relatively high (uncorrected *p*-distance 8.2%).

Based on our material, the two new species occur in sympatry in the middle Ayeyarwady, between Bhamo and Mandalay: they were collected together at three sites. As the subtle differences in external appearance that distinguish them were initially overlooked in the field, we do not know whether or not they inhabit similar microhabitats within these areas. Differences in the shape of the premaxilla and the mesethmoid between *P. castor* and *P. pollux* (Fig. 5) may translate into differences in snout shape and potentially also jaw protrusability (via interaction with the kinethmoid), which could suggest differences in feeding behaviour or diet. Such differences could potentially reduce competition between individuals of the two species when they occur in syntopy. The slight differences in the shape of pharyngeal teeth noted between the two species (Figs. 6, 14) may also imply differences in diet. All samples were obtained at the beginning of wet season, with increasing water level, when fishes migrate to just-flooded areas. It is known that many species that have specialised food and habitat requirements when resources are scarce will become more eurytopic when resources become more abundant, as in inundated floodplains (e.g., Lowe-McConnell, 1975: 214). Observations in the dry season may show that the two species have different microhabitats and requirements.

Pethiyagoda et al. (2012) originally included 25 species in their newly established genus *Pethia.* Since then, 12 new species (including the two described herein) have been described (mostly from India), while others have been transferred to *Pethia* from other genera (Kottelat, 2013) and species previously in the synonymy have been re-validated (e.g., Knight, 2013), bringing the present inventory of species to 40. Excluding the two new species described herein, members of *Pethia* exhibit dark markings on the body that are variable in number, shape (spot, blotch, or bar), and position. The most common pattern appears to comprise two dark markings, including a smaller anterior (humeral) marking and a larger posterior (typically vertically elongate) marking on the caudal peduncle (e.g., see fig. 2 in Katwate et al., 2016, 2018). In some species, a third dark marking may be present on the body side below the dorsal fin, as in for example the type species *P. nigrofasciata* (e.g., Pethiyagoda, 1991: 108, 110), *P. phutunio* (e.g., Kullander & Fang, 2005: fig. 6; Britz, 2019: pl. 189), or *P. striata* (Atkore et al., 2015). *Pethia gelius*, and also the presumed close relative *P. canius*, exhibits an additional dark marking over the base of the anal fin (Knight, 2013; Britz, 2019). In other species, the anterior marking is barely visible or absent and the posterior marking on the caudal peduncle is prominent (e.g., *P. erythromycter*, *P. nankyweensis*, and *P. thelys*; Kullander, 2008; *P. aurea* Knight, 2013). Our purpose here is not to describe every detail of body colour pattern in *Pethia* but to emphasise the unique condition in *P. castor* and *P. pollux*, which are the only species of *Pethia* described to date that lack dark markings on the body.

Despite lacking such markings, *Pethia castor* and *P. pollux* exhibit the majority of characters listed in the diagnosis of *Pethia* by Pethiyagoda et al. (2012), including, for example: absence of barbels; last unbranched dorsal-fin ray stiffened and serrated (Fig. 7C, D); gill rakers simple (Figs. 6C, 14C); IO3 deep, partially overlapping the cheek and preopercle (Fig. 4); free uroneural absent; post-epiphysial fontanelle absent (Fig. 4A, D); lateral line incomplete; and 22–24 scales in lateral line scale row. In fact, only one of the approximately 14 diagnostic characters of *Pethia* provided by Pethiyagoda et al. (2012: 80–81) is lacking in *P. castor* and *P. pollux*, a colour pattern "consisting of a black blotch on caudal peduncle and frequently also other black blotches, spots or bars on side of body".

The generic placement of *Pethia castor* and *P. pollux* is corroborated by our investigation of a small data set of COI sequences. In the results of both the ML and MP analyses, *P. castor* and *P. pollux* are recovered as sister taxa and placed as the closest relative of the Ganga-Brahmaputran species *P. gelius* (Fig. 15). Each of these relationships is supported by high bootstrap support values in the ML analysis (98–100%) and high to moderate values in the MP analysis (61–97%). Though sequences for *P. canius* and *P. aureus* were not available for our study, based on general appearance, we expect both to be close relatives of *P. gelius* (e.g., see Knight, 2013) and by association, potentially also close relatives of *P. castor* and *P. pollux*. Four of these species (all but *P. aurea*) share a black marking at the anterior dorsal-fin base,

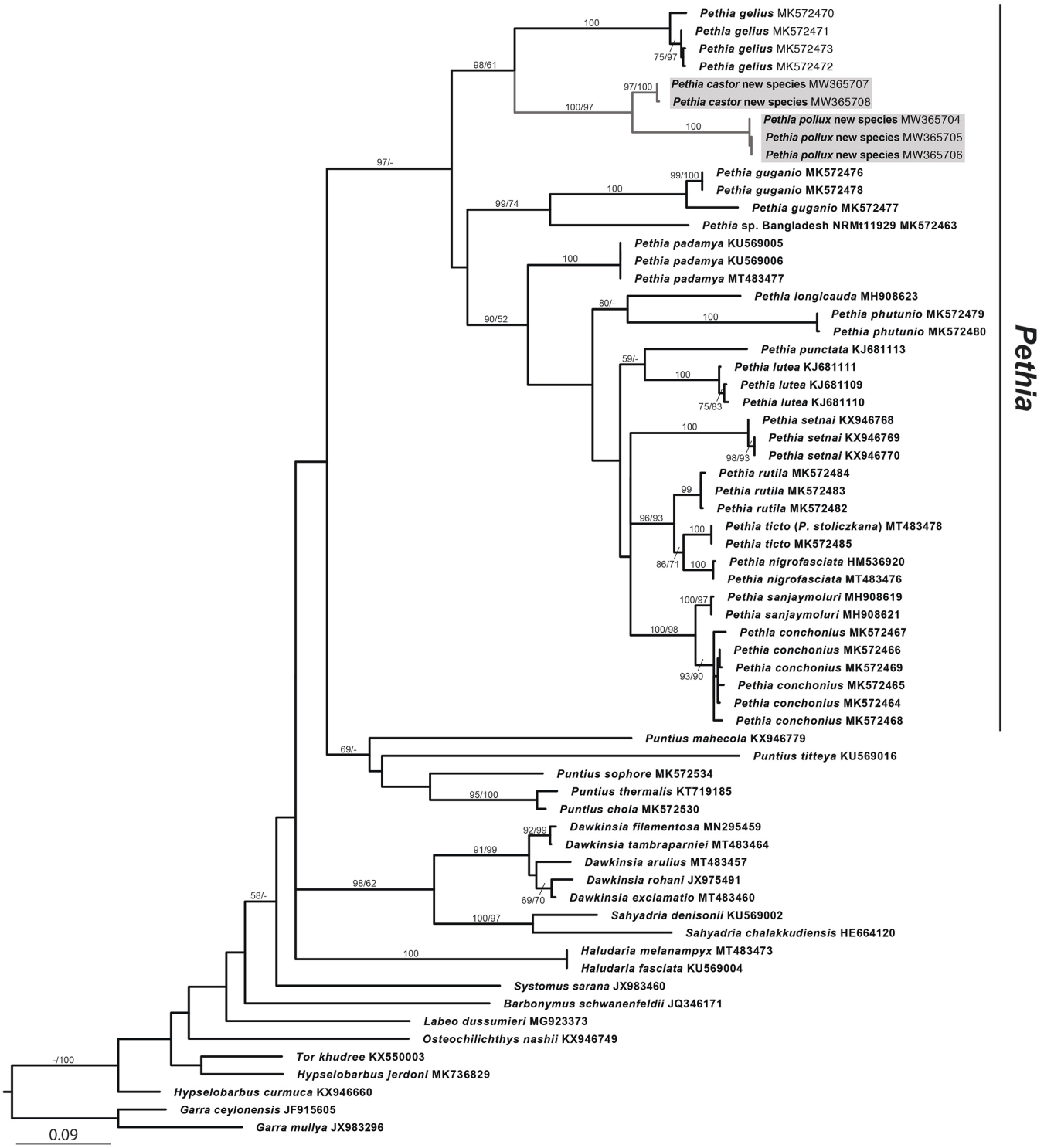

Fig. 15. Maximum likelihood (ML) phylogram with lowest log likelihood score (-In *L* -7149.3774) obtained from analysis of COI dataset showing phylogenetic position of new species (highlighted in grey boxes). Numbers above branches represent bootstrap values (>50%) associated with ML/Maximum Parsimony analyses.

obscuring the small anterior unbranched rays and also the base of the modified posterior unbranched ray. This marking is restricted to the fin in *P. castor* and *P. pollux* (Fig. 7A, B, D, E) but extends on to the body below the fin in *P. gelius* and *P. canius* (Britz, 2019: pls. 190, 191). To the best of our knowledge, this marking is unique to the aforementioned species of *Pethia* and may represent a synapomorphy of this clade (assuming character-loss in *P. aurea*).

The monophyly of *Pethia* is supported by high bootstrap support values in the ML analysis (97%) but not in the MP analysis (<50%) of our data set. Within the *Pethia* clade, the clade containing *P. gelius* and the two new species represents the sister taxon to a larger clade containing all remaining *Pethia* included in our data set (12 described and 1 undescribed species; Fig. 15; Appendix 1). This large clade of *Pethia* did not receive high bootstrap support, but

two subgroups within this clade are well supported with strong to moderate bootstrap support values, including *P. guganio*+*Pethia* sp. Bangladesh (99%[ML], 74%[MP]) and a 'core' clade containing the remaining 11 species (90%, 52%) (Fig. 15).

Katwate et al. (2014) too, used mitochondrial COI sequences to investigate phylogenetic relationships between 10 species of *Pethia*. Despite differences in taxon sampling, the topology presented by Katwate et al. (2014: fig. 3) and the topology presented herein (Fig. 15) are largely congruent. Katwate et al. (2014) recovered *P. gelius* as the sister taxon of the remaining members of *Pethia* (a group of eight species, though without bootstrap support). This clade of *Pethia*, including *P. padamya*, *P. phutunio*, *P. lutea*, *P. punctata*, *P. ticto*, *P. nigrofasciata*, *P. setnai*, and *P. conchonius*, is equivalent to the 'core' clade of *Pethia* recovered herein (including all of the aforementioned species plus *P. longicauda*, *P. rutila*, and *P. sanjaymoluri*). Comparing our results to those of the other phylogenetic investigations of *Pethia* conducted to date is difficult, and perhaps meaningless, because these other studies have relied on another mitochondrial gene (cytochrome b; Katwate et al., 2016) or a combination of multiple mitochondrial and nuclear genes (Ren et al., 2020). We make note here, however, that regardless of the data set used, the phylogenetic position of *P. gelius* is congruent across the various topologies recovered in these different studies (Katwate et al., 2014, 2016; Ren et al., 2020; Fig. 15 herein).

Based on the aforementioned relationships and the striking differences in colour pattern that exist between different species and/or lineages of the now sizable and morphologically variable *Pethia*, we foresee that it will not be long before it too, is carved up into a number of smaller genera, a recurring theme in taxonomic studies of Asian barbs (Rainboth, 1986, 1989, 1996; Pethiyagoda et al., 2012; Kottelat, 2013; Katwate et al., 2020).

ACKNOWLEDGEMENTS

Material of the new species was collected during surveys conducted with Fauna & Flora International (FFI), Myanmar Program. MK thanks U Myint Soe (retired director, Kachin State Department of Fisheries), and Myint Than Soe and Thet Yu Yu Swe (Department of Fisheries) for permission, assistance in the field trip and export permit, and Zau Lunn and Nyein Chan (FFI) for their help in the field. We thank K. D. Keith for calculating uncorrected P-distances, A. Summers for providing access to CT scanning equipment, R. Pethiyagoda, H. Sudasinghe and R. Britz for critical comments on an earlier draft of the manuscript, and R. Covain (MHNG), H. Prestridge (TCWC), R. Robins (UF), and K. Lim (ZRC) for registering and/or access to material. KWC and AKP were funded by Texas A&M Agrilife Research (TEX09452 to KWC). CT scanning was possible via funding from NSF (DBI 1702442 to KWC; DBI 1701665 to A. Summers at University of Washington) and the TAMU Innovation[X] 2020–21 project "Computer Tomography (CT) Technology Driving Innovative and Creative Uses of Natural History Collections Across Disciplines" (to H. Prestridge, TCWC). This is publication number 1631 of the Biodiversity Research and Teaching Collections at Texas A&M University.

LITERATURE CITED

Atkore VM, Knight JM, Devi KR & Krishnaswamy J (2015) A new species of *Pethia* from the Western Ghats, India (Teleostei: Cyprinidae). Copeia, 103: 290–296.

Batuwita S, Maduwage K & Sudasinghe H (2015) Redescription of *Pethia melanomaculata* (Teleostei: Cyprinidae) from Sri Lanka. Zootaxa, 3936: 575–583.

Britz R (2019) Francis Hamilton's Gangetic Fishes in colour. A new edition of the 1822 monograph, with reproductions of unpublished coloured illustrations. Ray Society, London: 1–48, i–vii, 1–405, i–vii, pls. 1–228.

Collins RA, Armstrong KF, Meier R, Yi Y, Brown SDJ, Cruickshank RH, Keeling S & Johnston C (2012) Barcoding and border biosecurity: identifying cyprinid fishes in the aquarium trade. PLoS ONE, 7: e28381.

Conway KW (2011) Osteology of the South Asian genus *Psilorhynchus* McClelland, 1839 (Teleostei: Ostariophysi: Psilorhynchidae), with investigation of its phylogenetic relationships within the order Cypriniformes. Zoological Journal of the Linnean Society, 163: 150–154.

Felsenstein J (1985) Confidence limits on phylogenies: an approach using the bootstrap. Evolution, 39(4): 783–791.

Folmer O, Black M, Hoeh W, Lutz R & Vrijenhoek R (1994) DNA primers for amplification of mitochondrial cytochrome c oxidase subunit I from diverse metazoan invertebrates. Molecular Marine Biology and Biotechnology, 3: 294–299.

Katwate U, Jadhav S, Kumkar P, Raghavan R & Dahanukar N (2016) *Pethia sanjaymoluri*, a new species of barb (Teleostei: Cyprinidae) from the northern Western Ghats, India. Journal of Fish Biology, 88: 2027–2050.

Katwate U, Katwate C, Raghavan R, Paingankar MS & Dahanukar N (2014) *Pethia lutea*, a new species of barb (Teleostei: Cyprinidae) and new records of *P. punctata* from northern Western Ghats of India. Journal of Threatened Taxa, 6: 5797–5818.

Katwate U, Kumkar P, Raghavan R & Dahanukar N (2018) A new syntopic species of small barb from the Western Ghats of India (Teleostei: Cyprinidae). Zootaxa, 4434: 529–546.

Katwate U, Kumkar P, Raghavan R & Dahanukar N (2020) Taxonomy and systematics of the 'Maharaja Barbs' (Teleostei: Cyprinidae), with the description of a new genus and species from the Western Ghats, India. Zootaxa, 4803: 544–560.

Katwate U, Raghavan R & Dahanukar N (2015) The identity of Hamilton's Ticto Barb, *Pethia ticto* (Teleostei: Cyprinidae). Zootaxa, 3964: 401–418.

Khedkar GD, Jamdade R, Naik S, David L & Haymer D (2014) DNA barcodes for the fishes of the Narmada, one of India's longest rivers. PloS one, 9: e101460.

Knight JDM (2013) *Pethia aurea* (Teleostei: Cyprinidae), a new species of barb from West Bengal, India, with redescription of *P. gelius* and *P. canius*. Zootaxa, 3700: 173–184.

Kottelat M (2001) Fishes of Laos. Wildlife Heritage Trust, Colombo, 198 pp.

Kottelat M (2013) The fishes of the inland waters of southeast Asia: a catalogue and core bibliography of the fishes known to occur in freshwaters, mangroves and estuaries. Raffles Bulletin of Zoology, Supplement 27: 1–663.

Kottelat M (2015) Fish species observed in Lenya River Drainage in Tanintharyi Region, in November 2014. Report No. 29 of the Tanintharyi Conservation Program, a joint initiative of Fauna & Flora International (FFI) and the Myanmar Government. FFI, Yangon.

Kottelat M & Nyein Chan (2017) Fish species observed in Middle Ayeyarwady in June–July 2017. Report No. 80 of the Myanmar Conservation and Development Programme, a joint initiative of Fauna & Flora International (FFI) and the Myanmar Government. FFI, Yangon.

Kullander SO (2008) Five new species of *Puntius* from Myanmar (Teleostei: Cyprinidae). Ichthyological Exploration of Freshwaters, 19: 59–84.

Kullander SO & Britz R (2008) *Puntius padamya*, a new species of cyprinid fish from Myanmar (Teleostei: Cyprinidae). Electronic Journal of Ichthyology, 4: 56–66.

Kullander SO & Fang F (2005) Two new species of *Puntius* from northern Myanmar (Teleostei: Cyprinidae). Copeia, 2005: 290–302.

Kumar S, Stecher G, Li M, Knyaz C & Tamura K (2018) MEGA X: Molecular Evolutionary Genetics Analysis across computing platforms. Molecular Biology and Evolution, 35: 1547–1549.

Lowe-McConnell RH (1975) Fish communities in tropical freshwaters – their distribution, ecology and evolution. Longman, London & New York, xviii + 337 pp.

Pasco-Viel E, Veran M & Viriot L (2012) Bleeker was right: Revision of the genus *Cyclocheilichthys* (Bleeker 1859) and resurrection of the genus *Anematichthys* (Bleeker 1859), based on morphological and molecular data of Southeast Asian Cyprininae (Teleostei, Cypriniformes). Zootaxa, 3586: 41–54.

Patil TS, Jamdade RA, Patil SM, Govindwar SP & Muley DV (2018) DNA barcode based delineation of freshwater fishes from northern Western Ghats of India, one of the world's biodiversity hotspots. Biodiversity and Conservation, 27: 3349–3371.

Pethiyagoda R (1991) Freshwater fishes of Sri Lanka. Wildlife Heritage Trust of Sri Lanka, Colombo, xiv + 362 pp.

Pethiyagoda R, Meegaskumbura M & Maduwage K (2012) A synopsis of the South Asian fishes referred to *Puntius* (Pisces: Cyprinidae). Ichthyological Exploration of Freshwaters, 23: 69–95.

Rahman MM, Norén M, Mollah AR & Kullander SO (2019) Building a DNA barcode library for the freshwater fishes of Bangladesh. Scientific Reports, 9: 1–10.

Rainboth WJ (1986) Fishes of the Asian cyprinid genus *Chagunius*. Occasional Papers of the Museum of Zoology, University of Michigan, 712: 1–17.

Rainboth WJ (1989) *Discherodontus*, a new genus of cyprinid fishes from southeastern Asia. Occasional Papers of the Museum of Zoology, University of Michigan, 718: 1–31.

Rainboth WJ (1991) Cyprinids of South East Asia. In: Winfield IJ & Nelson JS (eds.) Cyprinid fishes – Systematics, biology and exploitation. Chapman & Hall, London. Pp. 156–210.

Rainboth WJ (1996) The taxonomy, systematics, and zoogeography of *Hypsibarbus*, a new genus of large barbs (Pisces, Cyprinidae) from the rivers of southeastern Asia. University of California Publications, Zoology, 129: i–xiii + 1–199.

Raja M & Perumal P (2017) DNA barcoding and phylogenetic relationships of selected south Indian freshwater fishes based on mtDNA COI sequences. Journal of Phylogenetics and Evolutionary Biology, 5: 184.

Ren Q, Yang L, Chang CH & Mayden RL (2020) Molecular phylogeny and divergence of major clades in the *Puntius* complex (Teleostei: Cypriniformes). Zoologica Scripta, 49: 697–709.

Shangningam B & Vishwanath W (2018) *Pethia poiensis*, a new species of cyprinid fish from the Chindwin Basin of Manipur, India. Zootaxa, 4379: 585–593.

Stecher G, Tamura K & Kumar S (2020) Molecular Evolutionary Genetics Analysis (MEGA) for macOS. Molecular Biology and Evolution, 37(4): 1237–1239. doi: 10.1093/molbev/msz312

Swofford DL (2003) PAUP*. Phylogenetic Analysis Using Parsimony (*and other methods). Version 4. Sinauer Associates, Sunderland, Massachusetts.

Taki Y, Katsuyama A & Urushido T (1978) Comparative morphology and interspecific relationships of the cyprinid genus *Puntius*. Japanese Journal of Ichthyology, 25: 1–8.

Taylor WR & Van Dyke GC (1985) Revised procedures for staining and clearing small fishes and other vertebrates for bone and cartilage study. Cybium, 9: 107–119.

van der Walt KA, Mäkinen T, Swartz ER & Weyl OLF (2017) DNA barcoding of South Africa's ornamental freshwater fish–are the names reliable? African Journal of Aquatic Science, 42: 155–160.

Yang L, Mayden RL, Sado T, He S, Saitoh K & Miya M (2010) Molecular phylogeny of the fishes traditionally referred to Cyprinini sensu stricto (Teleostei: Cypriniformes). Zoologica Scripta, 39: 527–550.

Zwickl DJ (2006) Genetic algorithm approaches for the phylogenetic analysis of large biological sequence datasets under the maximum likelihood criterion. PhD Dissertation, The University of Texas at Austin, x + 115 pp.

APPENDIX

Appendix 1. GenBank numbers for COI sequences used in this study.

Species	GenBank Number	Locality/Source
Pethia pollux (CMK 27937)	MW365704	Myanmar: Kachin State/**this study**
Pethia pollux (CMK 27070)	MW365705	Myanmar: Kachin State/**this study**
Pethia pollux (CMK 27070)	MW365706	Myanmar: Kachin State/**this study**
Pethia castor (CMK 28806)	MW365707	Myanmar: Kachin State/**this study**
Pethia castor (CMK 28806)	MW365708	Myanmar: Kachin State/**this study**
Pethia conchonius	MK572469	Bangladesh: Chittagong Division, Bandarban District/Rahman et al. (2019)
Pethia conchonius	MK572468	Bangladesh: Chittagong Division/Rahman et al. (2019)
Pethia conchonius	MK572467	Bangladesh: Dhaka Division/Rahman et al. (2019)
Pethia conchonius	MK572466	Bangladesh: Chittagong Division/Rahman et al. (2019)
Pethia conchonius	MK572465	Bangladesh: Chittagong Division, Rangamati District/Rahman et al. (2019)
Pethia conchonius	MK572464	Bangladesh: Rangpur Division, Dinajpur District/Rahman et al. (2019)
Pethia gelius	MK572473	Bangladesh: Dhaka Division/Rahman et al. (2019)
Pethia gelius	MK572472	Bangladesh: Sylhet District/Rahman et al. (2019)
Pethia gelius	MK572471	Bangladesh: Mymenshing, Sherpur/Rahman et al. (2019)
Pethia gelius	MK572470	Bangladesh: Dhaka Division/Rahman et al. (2019)
Pethia guganio	MK572478	Bangladesh: Chittagong Division, Bandarban District/Rahman et al. (2019)
Pethia guganio	MK572477	Bangladesh: Dhaka Division/Rahman et al. (2019)
Pethia guganio	MK572476	Bangladesh: Chittagong Division/Rahman et al. (2019)
Pethia longicauda	MH908623	India: northern Western Ghats/unpublished
Pethia lutea	KJ681111	India: Sangameshwar, Ratnagiri District/Katwate et al. (2014)
Pethia lutea	KJ681110	India: Karjat/Katwate et al. (2014)
Pethia lutea	KJ681109	India: Bhira, Raigad District/Katwate et al. (2014)
Pethia nigrofasciata	MT483476	Locality not reported/Ren et al. (2020)
Pethia nigrofasciata	HM536920	Locality not reported/Yang et al. (2010)
Pethia padamya	KU569006	Aquarium trade/van Der Walt et al. (2017)
Pethia padamya	KU569005	Aquarium trade/van Der Walt et al. (2017)
Pethia padamya	MT483477	Locality not reported/Ren et al. (2020)
Pethia phutunio	MK572480	Bangladesh: Mymenshing, Sherpur/Rahman et al. (2019)
Pethia phutunio	MK572479	Bangladesh: Sylhet Division, Moulovibazar District/Rahman et al. (2019)
Pethia punctata	KJ681113	India: Madkhol/Katwate et al. (2014)
Pethia rutila	MK572484	Bangladesh: Chittagong Division, Cox's Bazar District/Rahman et al. (2019)
Pethia rutila	MK572483	Bangladesh: Chittagong Division, Cox's Bazar District/Rahman et al. (2019)
Pethia rutila	MK572482	Bangladesh: Chittagong Division/Rahman et al. (2019)
Pethia sanjaymoluri	MH908621	India: northern Western Ghats/unpublished
Pethia sanjaymoluri	MH908619	India: northern Western Ghats/unpublished
Pethia setnai	KX946770	India: Maharashtra, Kolhapur/Patil et al. (2018)

Species	GenBank Number	Locality/Source
Pethia setnai	KX946769	India: Maharashtra, Kolhapur/Patil et al. (2018)
Pethia setnai	KX946768	India: Maharashtra, Kolhapur/Patil et al. (2018)
Pethia ticto (as *Pethia stoliczkana)*	MT483478	Locality not reported/Ren et al. (2020)
Pethia ticto	MK572485	Bangladesh: Dhaka Division/Rahman et al. (2019)
Pethia sp. NRMt11929	MK572463	Bangladesh: Chittagong Division/Rahman et al. (2019)
Puntius chola	MK572530	Bangladesh: Rangpur Division, Dinajpur District/Rahman et al. (2019)
Puntius mahecola	KX946779	India: Maharashtra, Kolhapur/Patil et al. (2018)
Puntius sophore	MK572534	Bangladesh: Dhaka Division, Dhaka District/Rahman et al. (2019)
Puntius thermalis	KT719185	Sri Lanka/unpublished
Puntius titteya	KU569016	Aquarium trade/van Der Walt et al. (2017)
Dawkinsia arulius	MT483457	India/Ren et al. (2020)
Dawkinsia rohani	JX975491	Locality not reported/unpublished
Dawkinsia exclamatio	MT483460	India/Ren et al. (2020)
Dawkinsia tambraparniei	MT483464	India/Ren et al. (2020)
Dawkinsia filamentosa	MN295459	Locality not reported/unpublished
Haludaria melanampyx	MT483473	India/Ren et al. (2020)
Haludaria fasciata	KU569004	Aquarium trade/van Der Walt et al. (2017)
Sahyadria chalakkudiensis	HE664120	Locality not reported/unpublished
Sahyadria denisonii	KU569002	Aquarium trade/van Der Walt et al. (2017)
Systomus sarana	JX983460	India: Madhya Pradesh/Khedkar et al. (2014)
Tor khudree	KX550003	India/Raja & Perumal (2017)
Barbonymus schwanenfeldii	JQ346171	Laos/Pasco-Viel et al. (2012)
Hypselobarbus jerdoni	MK736829	India/unpublished
Hypselobarbus curmuca	KX946660	India: Maharashtra, Kolhapur/Patil et al. (2018)
Labeo dussumieri	MG923373	India: Kerala/unpublished
Osteochilichthys nashii	KX946749	India: Maharashtra, Kolhapur/Patil et al. (2018)
Garra ceylonensis	JF915605	Aquarium trade/Collins et al. (2012)
Garra mullya	JX983296	India: Madhya Pradesh/Khedkar et al. (2014)